

Fate of a multiple-band Fermi liquid that is coupled with critical ϕ^4 bosons

Zhiming Pan^{1,2} and Ryuichi Shindou^{1,2,*}

¹International Center for Quantum Materials, School of Physics, Peking University, Beijing 100871, China

²Collaborative Innovation Center of Quantum Matter, Beijing 100871, China

(Dated: March 21, 2022)

Multiple-band nature of electronic energy bands leads to novel physical effects in solids. In this Letter, we clarify physical properties of a Fermi system with a pair of electron and hole Fermi surfaces (FSs), whose coupling is mediated by a critical U(1) boson field. By using a one-loop renormalization group analysis, we show that when the boson field undergoes a quantum phase transition with broken U(1) symmetry, the multiple-band Fermi system shows a marginal Fermi liquid (FL) behaviour in its electromagnetic and thermodynamic properties. At a quantum critical point (QCP), Fermi velocities of the two FSs are renormalized into a same critical velocity as a boson velocity, and the fermion's density of states (DOS) shows a pseudo-gap behaviour at the QCP.

Experimental discoveries of graphene [1, 2] and topological insulators [3, 4] promote studies on unique physical effects that come from a multiple-band nature of electronic energy bands in solids [5–7]. The key ingredient in the recent studies is an interplay effect between the multiple-band nature and the other factors in solids, such as electron correlation, interaction with environments, disorder and so on [8–33]. During the last decade, theoretical works revealed novel interplay effects in Dirac and Weyl semimetal [34–37], together with experimental development of relevant materials [38]. Nonetheless, these fermions have zero (or tiny) density of states around the Fermi levels, where bulk electric transports are quantitatively tiny.

In this Letter, we study a multiple-band Fermi system with a finite volume of FS, that is coupled with a U(1) boson field in a ϕ^4 type action in (3+1)-dimension. We clarify that an interplay between the multiple-band nature and the many-body effect leads to a marginal Fermi liquid (FL) regime [39, 40] in its electronic phase diagram (Fig. 1). The Fermi system considered has an electron-type fermion (ψ_+) with an isotropic FS and hole-type fermion (ψ_-) with the same size of isotropic FS. The U(1) boson field ϕ mediates a coupling between the two FSs in a U(1) symmetric way; $\phi \rightarrow \phi e^{+2i\theta}$, $\psi_{\pm}^{\dagger} \rightarrow \psi_{\pm}^{\dagger} e^{\pm i\theta}$. We clarify how the Fermi system acquires a band gap when the boson system undergoes a quantum phase transition with the spontaneous symmetry breaking (SSB) of the U(1) symmetry. We uncover that the fermion's DOS shows a pseudo-gap behaviour at the QCP and physical properties exhibit unusual logarithmic T -dependences in a high-temperature (T) side of the QCP: see Table. I. The marginal FL discovered in this paper paves a solid path to future realizations of more exotic non-Fermi liquids [41–51] in multiple-band Fermi systems.

The boson system is described by the (3+1)-dimensional U(1) symmetric ϕ^4 action S_{ϕ} with the dy-

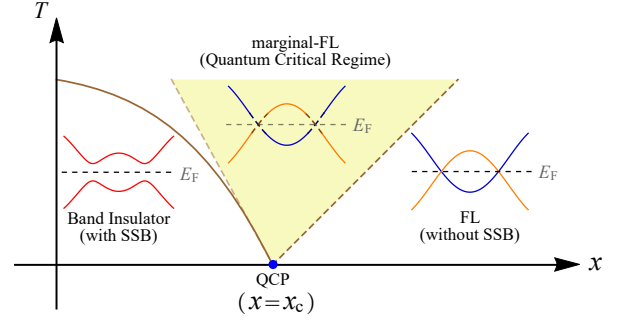


FIG. 1. A phase diagram of the two-band fermion system coupled with U(1) symmetric ϕ^4 boson: Eq. (1). The vertical axis is temperature T , and horizontal axis ($x \sim m_0^2$) is a parameter that induces a quantum phase transition with the SSB of the U(1) symmetry. In the SSB phase, the Fermi system acquires a finite band gap, while in the U(1) symmetric phase, the Fermi system belongs to a multiple-band Fermi liquid (m-FL) phase. At the QCP and its high- T side (QCR), the Fermi system shows a marginal-FL behaviour (See Table. I).

namical exponent $z = 1$,

$$\begin{cases} S_{\phi} = \int d^4x [m_0^2|\phi|^2 + |\partial_{\tau}\phi|^2 + c_0^2|\nabla_{\mathbf{x}}\phi|^2 + \frac{\lambda_0}{4}|\phi|^4], \\ S_{\psi} = \sum_{\sigma=\pm} \int_k \psi_{\sigma}^{\dagger}(k) [i\omega - \sigma v_{\sigma 0} l] \psi_{\sigma}(k), \\ S_{\text{int}} = g_0 \int_k \int_q [\phi^{\dagger}(q) \psi_{+}^{\dagger}(k) \psi_{-}(k+q) + \text{h.c.}], \end{cases} \quad (1)$$

with $x \equiv (\tau, \mathbf{x})$, a bare boson mass m_0^2 , boson velocity c_0 , and bare ϕ^4 coupling λ_0 . A fermion part of the action S_{ψ} is described by a spatially isotropic free theory with

	R	C_{el}/T	χ_{mag}	$1/(T_1 T)$	$\rho(\omega, T=0)$
marginal-FL	$\sqrt{ \ln T }$	$\frac{1}{\sqrt{ \ln T }}$	$\frac{1}{\sqrt{ \ln T }}$	$\frac{1}{ \ln T }$	$\frac{1}{\sqrt{ \ln \omega }}$

TABLE I. T -dependences of resistivity (R), specific heat C_{el} , and magnetic susceptibility χ_{mag} , and NMR relaxation time T_1 in the QCR and DOS near the Fermi level ($\omega = 0$) at the QCP. For the magnetic response, we consider a trivial SU(2) generalization of Eq. (1); $\psi_{\sigma} \rightarrow \psi_{\sigma,s}$, $\phi \psi_{-}^{\dagger} \psi_{+} \rightarrow \phi \psi_{-,s}^{\dagger} \psi_{+,s}$ with spin-1/2 $s = \uparrow, \downarrow$.

the dynamical exponent $z = 1$ with

$$\begin{cases} \int_k \equiv k_F^2 \int \frac{d^2 \hat{\Omega}}{(2\pi)^2} \int_{-\Lambda_F}^{\Lambda_F} \frac{d\omega}{2\pi} \int_{-\Lambda_F}^{\Lambda_F} \frac{dl}{2\pi}, \\ \int_q \equiv \int_{|\mathbf{q}| < \Lambda_B} \frac{d^3 \mathbf{q}}{(2\pi)^3} \int_{-\Lambda_B}^{\Lambda_B} \frac{d\varepsilon}{2\pi}. \end{cases} \quad (2)$$

Here k is fermion frequency and momentum; $k \equiv (\omega, \mathbf{k})$, $\mathbf{k} \equiv (k_F + l)\hat{\Omega}$, $|\hat{\Omega}| = 1$. v_{+0} and v_{-0} are bare fermion velocities of electron-type (ψ_+) and hole-type (ψ_-); $v_{+0} > 0$, $v_{-0} > 0$. The chemical potential is fine-tuned to a ‘charge neutrality point (CNP)’, with two identical isotropic FSs of the electron and hole-types. k_F is Fermi wavelength of the FS. A unit vector $\hat{\Omega}$ defines a direction of \mathbf{k} and a perpendicular component l defines a vertical distance of \mathbf{k} from the FS. q is boson frequency and momentum; $q \equiv (\varepsilon, \mathbf{q})$. Λ_F , $\bar{\Lambda}_F$, Λ_B and $\bar{\Lambda}_B$ are ultraviolet (UV) cutoff for l , ω , and q respectively. The fermion-boson coupling S_{int} is given by the Yukawa-type coupling with a bare coupling constant g_0 .

A ground state phase diagram of the coupled system possibly comprises of two phases; the SSB phase with $\langle \psi_+^\dagger \psi_- \rangle \neq 0$ (band insulator phase) and U(1) symmetric phase (multiple-band FL phase). At the exact CNP, the polarization function in an interband channel (Fig. 2(b)) has an infrared (IR) logarithmic singularity. The singularity in combination with any small Yukawa coupling g_0 could result in the low- T band insulator phase with the SSB. A transition temperature T_c is exponentially small for small g_0 ; $\log[T_c/\bar{\Lambda}_F] \propto -1/g_0^2$. In actual physical systems, the IR logarithmic singularity is regularized by other effects in low-energy scale. Such are disorder and static inhomogeneity (e.g. an uncontrolled deviation from the CNP). Using these IR regularizations implicitly, we assume the presence of the multiple-band FL phase and the quantum critical point (QCP) between the FL and the band insulator phases (Fig. 1). Thereby, the phase transition between the two is primarily driven by a change of the boson mass. In the following, we will uncover universal properties at such QCP and in a high- T side of the QCP (quantum critical regime; QCR).

To this end, let us begin with a general consideration on renormalizability of the effective model in Eq. (1). For Eq. (1), vertex functions have potentially UV divergences in the power of the large UV cutoff Λ ($\Lambda = \Lambda_B, \bar{\Lambda}_B, \Lambda_F, \bar{\Lambda}_F$). Denote as M the degree of the UV divergence of the vertex function $\Gamma^{(N_F, N_B)}$ with N_F and N_B external fermion and boson lines respectively. M can be superficially evaluated by dimensional countings, and it is bounded from above by $M \leq 4 - \frac{3}{2}N_F - N_B$. That says, the effective model in the (3+1)-dimension is renormalizable, where only the following four vertex functions have the UV divergences in Λ [52];

$$\begin{cases} \Gamma_\sigma^{(2,0)}(i\omega, \mathbf{k}) = \dots \Lambda + \dots \ln \Lambda i\omega + \dots \ln \Lambda l, \\ \Gamma^{(0,2)}(i\varepsilon, \mathbf{q}) = \dots \Lambda^2 + \dots \ln \Lambda \varepsilon^2 + \dots \ln \Lambda \mathbf{q}^2, \\ \Gamma_\sigma^{(2,1)}(\dots) = \dots \ln \Lambda + \mathcal{O}(\omega, l, q), \\ \Gamma^{(0,4)}(\dots) = \dots \ln \Lambda + \mathcal{O}(\omega, l, q). \end{cases} \quad (3)$$

Here the subscript $\sigma = \pm$ is a band index, that distinguishes different functions for the same N_F and N_B . Thereby, we will use the standard renormalized perturbation theory, and eliminate all the UV divergences in Eq. (3) by absorbing them into renormalizations of field operator amplitudes, and physical measurable quantities. As shown in the supplemental materials [52], the Λ -linear divergence in $\Gamma^{(2,0)}$ does not appear in the actual perturbation calculation. We thus consider only the renormalizations of field operator amplitudes, velocities, boson mass, Yukawa and ϕ^4 couplings, while taking the Fermi wavelength to be always k_F .

The effective model assumes that $q, \omega, l \ll \Lambda \ll k_F$. By the renormalized perturbation theory, the set of renormalized vertex functions shall be free from the UV cutoff Λ ; the Λ -divergent terms in Eq. (3) are absorbed into the renormalizations of the physical quantities and field operator amplitudes, while q/Λ , ω/Λ , l/Λ are set to zero in renormalized functions. On the one hand, the renormalized vertex functions thus obtained depend not only on q , ω , l but also on k_F . Such an exceptional treatment of k_F in spite of $q, \omega, l \ll \Lambda \ll k_F$ becomes possible, because all the vertex functions in Eq. (3) can be expanded in the power of k_F^2 [52]. Namely, it generally holds true for $N_F = 0, 2$ that $\Gamma^{(N_F, N_B)} = \Gamma^{(N_F, N_B; 0)} + k_F^2 \Gamma^{(N_F, N_B; 1)} + \dots$, where $k_F^{2n} \Gamma^{(N_F, N_B; n)}$ is a sum of all those amputated 1-particle irreducible (1PI) Feynman diagrams for $\Gamma^{(N_F, N_B)}$ with n numbers of internal closed fermion loops. Importantly, $\Gamma^{(N_F, N_B; n)}$ has no k_F -dependence and their k_F -dependence appear only through the overall factor k_F^{2n} . Thanks to this analytic nature as functions of k_F^2 , the UV divergences in Eq. (3) can be removed at every order in k_F^2 . In $\Gamma^{(N_F, N_B; n)}$ thus given, the superficial degree of the UV divergence in the power of Λ is smaller than that of $\Gamma^{(N_F, N_B; 0)}$ by $2n$. Accordingly, we have only to keep track of the first order in k_F^2 of $\Gamma^{(0,2)}$; see Eq. (3).

To eliminate the UV divergent terms in Eq. (3), we impose the following renormalization conditions on $\bar{\Gamma}^{(N_F, N_B)}$. $\bar{\Gamma}^{(N_F, N_B)}$ is a renormalized vertex function of $\Gamma^{(N_F, N_B)}$. The conditions read

$$\begin{cases} \bar{\Gamma}_\sigma^{(2,0)}(\omega = l = 0) = 0, \quad \left. \frac{\partial \bar{\Gamma}_\sigma^{(2,0)}(\omega, l)}{\partial (i\omega)} \right|_{v_\sigma l=0, \omega=\kappa} = 1, \\ \left. \frac{\partial \bar{\Gamma}_\sigma^{(2,0)}(\omega, l)}{\partial (v_\sigma l)} \right|_{v_\sigma l=\kappa, \omega=0} = -\sigma, \\ \bar{\Gamma}^{(0,2)}(\varepsilon = \kappa, \mathbf{q} = 0) = m^2 + \kappa^2, \\ \left. \frac{\partial \bar{\Gamma}^{(0,2)}(q)}{\partial \varepsilon} \right|_{\mathbf{q}=0, \varepsilon=\kappa} = 2\kappa + \frac{g^2}{\pi^2(v_+ + v_-)} \frac{k_F^2}{\kappa}, \\ \left. \frac{\partial \bar{\Gamma}^{(0,2)}(q)}{\partial (c|\mathbf{q}|)} \right|_{c|\mathbf{q}|=\kappa, \varepsilon=0} = 2\kappa + \frac{g^2}{\pi^2(v_+ + v_-)} \frac{k_F^2}{\kappa}, \\ \bar{\Gamma}_\sigma^{(2,1)}(\dots) = -g, \quad \bar{\Gamma}^{(0,4)}(\dots) = -\lambda, \end{cases} \quad (4)$$

with $\sigma = \pm$. κ in Eq. (4) is an external momentum and frequency of the functions, at which the conditions are imposed. The right hand sides of Eq. (4) are free from the UV cutoff Λ , and they depend only on physical

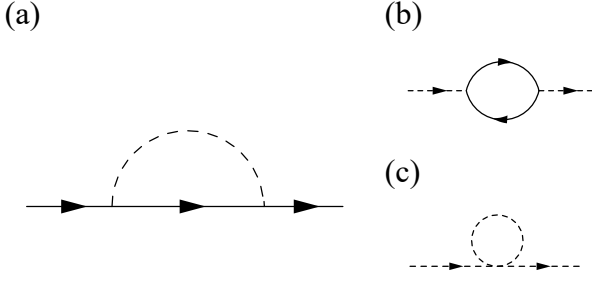


FIG. 2. (a-c) One-loop corrections included in the perturbative renormalization theory analysis. Solid/broken line represent fermion/boson lines respectively.

measurable quantities such renormalized boson mass m , renormalized Fermi velocities v_{\pm} , boson velocity c , and renormalized coupling constants g , λ . When the renormalized mass is set to the zero (at the critical point), Λ finite ' κ ' controls infrared behaviours of the functions. In accordance with the expansion of $\Gamma^{(0,2)}$ in k_F^2 , the conditions for $\bar{\Gamma}^{(0,2)}$ are expanded in the power of k_F^2 up to the first order.

In terms of minimal substraction scheme [53, 54], the renormalized vertex functions are made to satisfy the conditions perturbatively in the coupling constants, g and λ . The perturbative treatment will be a posteriori justified by β -functions of g and λ . A general relation among numbers of internal integral variables, g and λ in a vertex function suggests that g^2 and λ should be treated as the same order [52]. Under Eq. (4), all the UV divergences in the vertex functions in Eq. (3) are absorbed into bare quantities ($v_{\sigma 0}$, m_0^2 , c_0 , g_0 , λ_0) and renormalizations of field operator amplitudes (Z_{σ} , Z_{ϕ}),

$$v_{\sigma 0} = v_{\sigma} + \frac{g^2(v_{\sigma} - c)}{4\pi^2 c^2(c + v_{\bar{\sigma}})} \log\left(\frac{\Lambda_B}{\kappa}\right) + \dots, \quad (5)$$

$$Z_{\sigma} = 1 - \frac{g^2}{4\pi^2 c^2(c + v_{\bar{\sigma}})} \log\left(\frac{\Lambda_B}{\kappa}\right) + \dots, \quad (6)$$

$$m_0^2 = \frac{g^2 k_F^2}{\pi^2(v_+ + v_-)} \log\left(\frac{\Lambda_F}{\kappa}\right) - \frac{\lambda \Lambda_B^2}{16\pi^2 c^3} + \dots, \quad (7)$$

$$g_0 = g + \frac{g^3}{8\pi^2 c^2} \frac{2c + v_+ + v_-}{(c + v_+)(c + v_-)} \log\left(\frac{\Lambda_B}{\kappa}\right) + \dots, \quad (8)$$

$$\lambda_0 = \lambda + \frac{5\lambda^2}{16\pi^2 c^3} \log\left(\frac{\Lambda_B}{\kappa}\right) + \dots, \quad (9)$$

with $c_0 = c + \dots$, $Z_{\phi} = 1 + \dots$, $\bar{\sigma} = \mp$ for $\sigma = \pm$. Here only the leading order terms in g^2 and λ that depend on either Λ or κ are shown explicitly in the right hand sides, while the others are omitted by ' \dots '. The renormalized vertex functions defined by renormalized field operators, $\bar{\psi}_{\sigma} \equiv \psi_{\sigma}/\sqrt{Z_{\sigma}}$, $\bar{\phi} \equiv \phi/\sqrt{Z_{\phi}}$, are free from the UV cutoff as functions of the renormalized physical quantities.

Several remarks on the set of the equations above are noted in the followings [52]. $\log \Lambda$ in $v_{\sigma 0}$, Z_{σ} and g_0 are from a UV logarithmic divergent term in the fermion

self-energy (Fig. 2(a)). They play the major role in the following argument. $\log \Lambda$ and Λ^2 in m_0^2 are from the divergent terms in the boson self-energy with an internal fermion and boson loop respectively; Fig. 2(b) and Fig. 2(c). $\log \Lambda$ in λ_0 comes from a 1-loop correction to $\Gamma^{(0,4)}$. In this work, we consider to carry out the renormalization at the quantum critical point and set $m = 0$ in Eq. (4). Eq. (7) defines a subspace of $m = 0$ (quantum critical 'point') in a multiple-parameter space subtended by the bare quantities and $\ln \kappa$. When $m = 0$, the external momenta κ plays role of the renormalization group (RG) scale variable and all the $\log \Lambda$ in the above equations come in pairs with $-\log \kappa$.

Marginal FL features around QCP are encoded in the renormalized two-point fermion vertex functions. To decode them, let us begin with Callan-Symanzik (CS) equation for the renormalized fermion vertex functions [52];

$$\left\{ \frac{\partial}{\partial \ln \kappa} + \sum_{\sigma'=\pm} \beta_{v_{\sigma'}} \frac{\partial}{\partial v_{\sigma'}} + \beta_g \frac{\partial}{\partial g} + \beta_{\lambda} \frac{\partial}{\partial \lambda} - \gamma_{\sigma} \right\} \bar{\Gamma}_{\sigma}^{(2,0)}(l, \omega; c, \dots, \lambda, \kappa) = \frac{\partial m_0^2}{\partial \ln \kappa} \frac{\partial \Gamma_{\sigma}^{(2,0)}}{\partial m_0^2} \quad (10)$$

with β functions of Fermi velocities, and coupling constants,

$$\begin{cases} \beta_{v_{\sigma}} \equiv \frac{\partial v_{\sigma}}{\partial \ln \kappa} \Big|_{c_0, \dots, \Lambda} = \frac{g^2}{4\pi^2 c(c + v_{\bar{\sigma}})} \left(\frac{v_{\sigma}}{c} - 1 \right) + \dots, \\ \beta_g \equiv \frac{\partial g}{\partial \ln \kappa} \Big|_{c_0, \dots, \Lambda} = \frac{g^3}{8\pi^2 c^2} \left(\frac{1}{c + v_+} + \frac{1}{c + v_-} \right) + \dots \\ \beta_{\lambda} \equiv \frac{\partial \lambda}{\partial \ln \kappa} \Big|_{c_0, \dots, \Lambda} = \frac{5\lambda^2}{16\pi^2 c^3} + \dots, \end{cases} \quad (11)$$

and γ functions of the two fermion bands ($\sigma = \pm$),

$$\gamma_{\sigma} \equiv \frac{\partial \ln Z_{\sigma}}{\partial \ln \kappa} \Big|_{c_0, \dots, \Lambda} = \frac{g^2}{4\pi^2 c^2(c + v_{\bar{\sigma}})} + \dots. \quad (12)$$

The β functions of the velocities show that two Fermi velocities v_{\pm} are renormalized into the boson velocity c in the infrared (IR) limit ($\kappa \rightarrow 0$). This suggests that v_{\pm} in the CS equation could be set to c in the low-energy limit (see below). β functions of the coupling constants dictate that the two coupling constants are marginally irrelevant in the IR limit. The marginal irrelevance justifies a posteriori the perturbative treatment of the coupling constants.

To solve the CS equation in favor for the vertex functions, note also that the right hand side of Eq. (10) is on the higher order in the coupling constants, $\mathcal{O}(g^4)$, because $\partial m_0^2 / \partial \ln \kappa \propto \mathcal{O}(g^2)$ and $\partial \Gamma_{\sigma}^{(2,0)} / \partial m_0^2 \propto \mathcal{O}(g^2)$ [52]. Thus, the equation can be approximated by the homogeneous form in the leading order. Besides, the λ -dependence of $\bar{\Gamma}^{(2,0)}$ must start from the order of $\mathcal{O}(g^2 \lambda)$, so that $\partial \lambda$ in Eq. (10) leads to the higher-order terms, $\mathcal{O}(g^2 \lambda^2)$, and can be omitted. These simplifications with

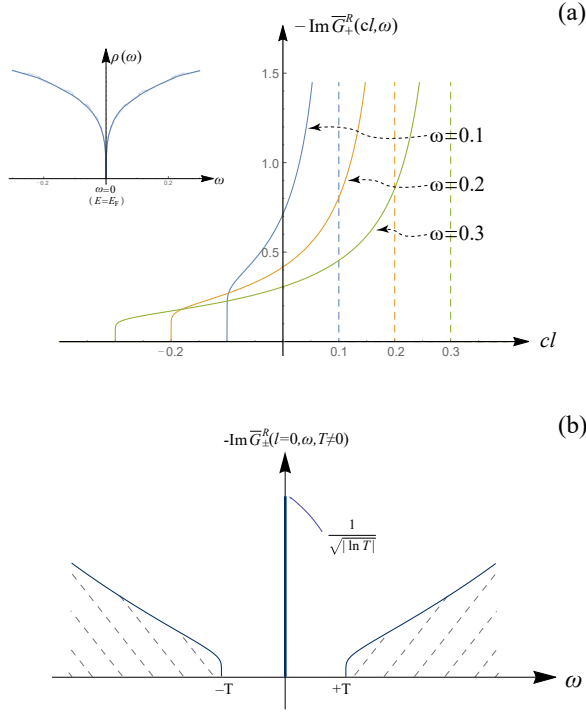


FIG. 3. (a) Renormalized spectral function for the electron-type band at the QCP: $-\text{Im}G_+^R(cl, \omega)$ is plotted as a function of cl for $\omega = 0.1, 0.2, 0.3$ with the RG scale $\kappa = 1$. (inset) DOS at the QCP: $\rho(\omega)$. (b) Renormalized spectral function on the FS ($cl = 0$) at finite T .

$v_{\pm} = c$ lead to the homogeneous CS equation with one-parameter scaling;

$$\left\{ \frac{\partial}{\partial \ln \kappa} + \beta_g \frac{\partial}{\partial g} - \gamma_{\sigma} \right\} \bar{\Gamma}_{\sigma}^{(2,0)}(l, \omega; g, \kappa) = 0. \quad (13)$$

The solution of the homogeneous CS equation is given in the form of the renormalized Green's function with $\bar{\Gamma}_{\sigma}^{(2,0)} \bar{G}_{\sigma}^{(2,0)} = 1$;

$$\bar{G}_{\sigma}^{(2,0)}(l, \omega; g, \kappa) = \frac{\exp \left[- \int_g^{\kappa} \frac{\gamma_{\sigma}(g')}{\beta_g(g')} dg' \right]}{i\omega - \sigma cl} = \frac{\bar{g}(t)}{i\omega - \sigma cl}. \quad (14)$$

$\bar{g}(t)$ with $t \equiv \log(\sqrt{\omega^2 + (cl)^2}/\kappa)$ is a solution of the one-parameter scaling equation; $\partial \bar{g}/\partial t = \beta_g(\bar{g})$, $\bar{g}(t=0) = g$,

$$\bar{g}(t) = g/\sqrt{1 - 2\alpha t}, \quad (15)$$

with $\alpha \equiv g^2/(8\pi^2 c^3)$. In Eq. (14), we used $\gamma_{\sigma}(g)/\beta_g(g) = 1/g$ from Eqs. (11,12) with $v_{\pm} = c$. After an analytic continuation, $i\omega \rightarrow \omega + i\delta$, Eq. (14) gives fermion retarded Green's function, spectral function and DOS at the QCP (Fig. 3(a)). Thereby, it can be clearly seen that the quasi-particle spectral weight at $T = 0$ is zero because \bar{g}/g in Eq. (14) goes to zero whenever $\omega \rightarrow \sigma cl$; Re $t \rightarrow -\infty$. The spectral function comprises of continuum spectrum, that shows an asymptotic form of

$1/[\eta |\ln \eta|^{\frac{3}{2}}]$ when $\omega = \sigma(cl + \eta)$ with small positive η . The asymptotic form around $\omega = \sigma cl$ plays major role in the pseudo-gap behaviour of the DOS at the QCP; $\rho(\omega) \propto 1/|\ln |\omega||^{\frac{3}{2}}$ (Fig. 3a) [52].

The T -dependences of the physical properties in the QCR can be obtained from those of the DOS ρ and quasi-particle life time τ on the FS. To determine them, we set $l = 0$ and replace t by $\log(\sqrt{\omega^2 + T^2}/\kappa)$ in Eqs. (14,15). The analytic continuation gives the retarded Green's function at finite- T on the FS;

$$\bar{G}_{\sigma}^{R,-1}(l=0, \omega, T \neq 0) = \sqrt{2\alpha} \left| \log \left(\frac{\sqrt{|T^2 - \omega^2|}}{\kappa} \right) \right|^{\frac{1}{2}} \times \left(\omega + \frac{\pi}{4} i \frac{|\omega| \theta(|\omega| - T)}{|\log(\sqrt{\omega^2 + T^2}/\kappa)|} \right) + \dots \quad (16)$$

The overall factor indicates that the quasi-particle spectral weight is finite at finite T and it scales as $1/|\ln T|^{\frac{1}{2}}$ (Fig. 3(b)). So does the DOS on the FS. The imaginary part inside the parentheses is zero at $\omega = 0$, indicating that the quasi-particle life time τ is determined by other effects in the low-energy scale. The most relevant effect in solids comes from electron scatterings by static impurities, which bring a finite life time at the low- T limit; τ is primarily T -independent, $\tau^{-1} = \tau_{\text{imp}}^{-1} + \mathcal{O}(T/|\log T|)$. The T -dependences of ρ and τ determine that of the electric resistivity through the Einstein relation, $R \propto |\log T|^{\frac{1}{2}}$, as well as the other properties in the QCR (Table I). From Eq. (16), the spectral function at $T \neq 0$ also has continuum spectrum at $|\omega| > T$, which shows a characteristic asymptotic form of $1/(T|\log \eta|^{\frac{3}{2}})$ when $|\omega| = T + \eta$ (Fig. 3(b)). Note that our theoretical analysis implicitly assumes the IR regularization due to disorder or inhomogeneity. These perturbations introduce a tiny but finite low-energy scale τ_0^{-1} , that imposes a low- T and/or ω boundaries of the theory applicability. Namely, the results summarized in Table I is valid for $\omega, T \gg \tau_0^{-1}$.

As for a physical lattice model to which Eq. (1) is applicable, a quantum rotor model (QRM) [55] coupled with a sp_+ model [56–58] is considered. The QRM comprises of a U(1) phase variable $\theta_{\mathbf{j}}$ and its canonical conjugate momentum $L_{\mathbf{j}}$, defined on a cubic lattice site \mathbf{j} ; For a heavier mass of the quantum rotor, the boson model undergoes a quantum phase transition to a long-range ordering of the U(1) phase variable. The sp_+ model is a tight-binding model on the cubic lattice, that has s -($s_{\mathbf{j}}$) and p_+ ($p_+ \equiv p_x + ip_y$ orbitals ($p_{\mathbf{j}}$) on the same lattice site \mathbf{j} . The sp_+ model has a pair of electron and hole pockets around high symmetric points. When the rotor is regarded as an electric/magnetic dipole moment, the simplest symmetry-allowed coupling between the rotor and the fermions is given by $e^{i\theta_{\mathbf{j}}} s_{\mathbf{j}}^{\dagger} p_{\mathbf{j}}$. Such an on-site coupling in combination with QRM and sp_+ model can be described by the effective model of Eq. (1) near the quantum phase transition point. Another physical application can be found in a 3-dimensional interacting Fermi

system with a pair of electron and hole FSs with a possible excitonic instability [52].

This work was supported by NBRP of China Grants No. 2015CB921104, No. 2017A040215 and No. 2019YFA0308401.

* rshindou@pku.edu.cn

- [1] K. S. Novoselov, A. K. Geim, S. V. Morozov, D. Jiang, K. M. I., I. V. Grigorieva, S. V. Dubonos, and A. A. Firsov, *Nature* **438**, 197 (2005).
- [2] Y. Zhang, Y. W. Tan, H. L. Stomer, and P. Kim, *Nature* **438**, 201 (2005).
- [3] M. König, S. Wiedmann, C. Brune, A. Roth, H. Buhmann, L. W. Molenkamp, X. L. Qi, and S. C. Zhang, *Science* **318**, 766 (2007).
- [4] D. Hsieh, D. Qian, L. Wray, Y. Xia, Y. S. Hor, R. J. Cava, and M. Z. Hasan, *Nature* **452**, 970 (2008).
- [5] D. Xiao, M.-C. Chang, and Q. Niu, *Rev. Mod. Phys.* **82**, 1959 (2010).
- [6] X.-L. Qi and S.-C. Zhang, *Rev. Mod. Phys.* **83**, 1057 (2011).
- [7] M. Z. Hasan and C. L. Kane, *Rev. Mod. Phys.* **82**, 3045 (2010).
- [8] A. H. Castro Neto, F. Guinea, N. M. R. Peres, K. S. Novoselov, and A. K. Geim, *Rev. Mod. Phys.* **81**, 109 (2009).
- [9] D. J. Gross and A. Neveu, *Phys. Rev. D* **10**, 3235 (1974).
- [10] I. F. Herbut, *Phys. Rev. Lett.* **97**, 146401 (2006).
- [11] F. F. Assaad and I. F. Herbut, *Phys. Rev. X* **3**, 031010 (2013).
- [12] A. V. Chubukov, D. V. Efremov, and I. Eremin, *Phys. Rev. B* **78**, 134512 (2008).
- [13] R. Fernandes, A. Chubukov, and J. Schmalian, *Nature Physics* **10**, 97 (2014).
- [14] K. Sun, H. Yao, E. Fradkin, and S. A. Kivelson, *Phys. Rev. Lett.* **103**, 046811 (2009).
- [15] E.-G. Moon, C. Xu, Y. B. Kim, and L. Balents, *Phys. Rev. Lett.* **111**, 206401 (2013).
- [16] L. Savary, E.-G. Moon, and L. Balents, *Phys. Rev. X* **4**, 041027 (2014).
- [17] M. Dzero, K. Sun, V. Galitski, and P. Coleman, *Phys. Rev. Lett.* **104**, 106408 (2010).
- [18] S. Wolgast, i. m. c. b. u. i. e. i. f. Kurdak, K. Sun, J. W. Allen, D.-J. Kim, and Z. Fisk, *Phys. Rev. B* **88**, 180405 (2013).
- [19] M. Neupane, N. Alidoust, S.-Y. Xu, T. Kondo, Y. Ishida, D. J. Kim, C. Liu, I. Belopolski, Y. J. Jo, T. R. Chang, H.-T. Jeng, T. Durakiewicz, L. Balicas, H. Lin, A. Bansil, S. Shin, Z. Fisk, and M. Z. Hasan, *Nature Communications* **4**, 2991 (2013).
- [20] J. Jiang, S. Li, T. Zhang, Z. Z. Sun, F. Chen, Z. R. Ye, M. Xu, Q. Q. Ge, S. Y. Tan, X. H. Niu, M. Xia, B. P. Xie, Y. F. Li, X. H. Chen, H. H. Wen, and D. L. Feng, *Nature Communications* **4**, 3010 (2013).
- [21] J. Li, R.-L. Chu, J. K. Jain, and S.-Q. Shen, *Phys. Rev. Lett.* **102**, 136806 (2009).
- [22] C. W. Groth, M. Wimmer, A. R. Akhmerov, J. Tworzydło, and C. W. J. Beenakker, *Phys. Rev. Lett.* **103**, 196805 (2009).
- [23] H. Jiang, L. Wang, Q.-f. Sun, and X. C. Xie, *Phys. Rev. B* **80**, 165316 (2009).
- [24] E. J. Meier, F. A. An, A. Dauphin, M. Maffei, P. Massignan, T. L. Hughes, and B. Gadway, *Science* **362**, 929 (2018), <https://science.sciencemag.org/content/362/6417/929.full.pdf>.
- [25] S. Stutzer, Y. Plotnik, Y. Lumer, P. Titum, N. H. Lindner, M. Segev, M. C. Rechtsman, and A. Szameit, *Nature* **560**, 461 (2018).
- [26] S. Raghu, X.-L. Qi, C. Honerkamp, and S.-C. Zhang, *Phys. Rev. Lett.* **100**, 156401 (2008).
- [27] S. Rachel and K. Le Hur, *Phys. Rev. B* **82**, 075106 (2010).
- [28] F. D. M. Haldane, *Phys. Rev. Lett.* **93**, 206602 (2004).
- [29] R. Shindou and L. Balents, *Phys. Rev. Lett.* **97**, 216601 (2006).
- [30] R. Shindou and L. Balents, *Phys. Rev. B* **77**, 035110 (2008).
- [31] Z. Wang, X.-L. Qi, and S.-C. Zhang, *Phys. Rev. Lett.* **105**, 256803 (2010).
- [32] Z. Wang and S.-C. Zhang, *Phys. Rev. X* **2**, 031008 (2012).
- [33] J.-Y. Chen and D. T. Son, *Annals of Physics* **377**, 345 (2017).
- [34] P. Goswami and S. Chakravarty, *Phys. Rev. Lett.* **107**, 196803 (2011).
- [35] H. Isobe and N. Nagaosa, *Phys. Rev. B* **86**, 165127 (2012).
- [36] E. Fradkin, *Phys. Rev. B* **33**, 3263 (1986).
- [37] S. V. Syzranov and L. Radzihovsky, *Annual Review of Condensed Matter Physics* **9**, 35 (2018), <https://doi.org/10.1146/annurev-conmatphys-033117-054037>.
- [38] N. P. Armitage, E. J. Mele, and A. Vishwanath, *Rev. Mod. Phys.* **90**, 015001 (2018).
- [39] C. M. Varma, P. B. Littlewood, S. Schmitt-Rink, E. Abrahams, and A. E. Ruckenstein, *Phys. Rev. Lett.* **63**, 1996 (1989).
- [40] V. M. Yakovenko, *Phys. Rev. B* **47**, 8851 (1993).
- [41] P. A. Lee, *Phys. Rev. Lett.* **63**, 680 (1989).
- [42] B. L. Altshuler, L. B. Ioffe, and A. J. Millis, *Phys. Rev. B* **50**, 14048 (1994).
- [43] Y. B. Kim, A. Furusaki, X.-G. Wen, and P. A. Lee, *Phys. Rev. B* **50**, 17917 (1994).
- [44] W. Metzner, D. Rohe, and S. Andergassen, *Phys. Rev. Lett.* **91**, 066402 (2003).
- [45] J. Rech, C. Pépin, and A. V. Chubukov, *Phys. Rev. B* **74**, 195126 (2006).
- [46] E. Fradkin, S. A. Kivelson, M. J. Lawler, J. P. Eisenstein, and A. P. Mackenzie, *Annual Review of Condensed Matter Physics* **1**, 153 (2010), <https://doi.org/10.1146/annurev-conmatphys-070909-103925>.
- [47] S.-S. Lee, *Phys. Rev. B* **80**, 165102 (2009).
- [48] A. Abanov, A. V. Chubukov, and J. Schmalian, *Advances in Physics* **52**, 119 (2003), <https://doi.org/10.1080/0001873021000057123>.
- [49] M. A. Metlitski and S. Sachdev, *Phys. Rev. B* **82**, 075127 (2010).
- [50] M. A. Metlitski and S. Sachdev, *Phys. Rev. B* **82**, 075128 (2010).
- [51] A. L. Fitzpatrick, S. Kachru, J. Kaplan, and S. Raghu, *Phys. Rev. B* **88**, 125116 (2013).
- [52] See Supplemental Material at [URL will be inserted by publisher] for a general argument on the renormalizability of the effective model, perturbative renormalization theory analyses on the model, Callan-Symmanzik equa-

tions, the pseudo-gap behaviour of the DOS at the QCP, and physical applications of the effective model studied in the paper.

- [53] M. E. Peskin and D. V. Schroeder, *Introduction to Quantum Field Theory* (Westview, 1995).
- [54] D. J. Amit and V. Martin-Mayor, *Field Theory, Renormalization Group and Critical Phenomena* (World Scientific, 2005).
- [55] S. Sachdev, *Quantum Phase Transitions* (Cambridge University Press, 1999).
- [56] K.-Y. Yang, Y.-M. Lu, and Y. Ran, Phys. Rev. B **84**, 075129 (2011).
- [57] C.-Z. Chen, J. Song, H. Jiang, Q.-f. Sun, Z. Wang, and X. C. Xie, Phys. Rev. Lett. **115**, 246603 (2015).
- [58] S. Liu, T. Ohtsuki, and R. Shindou, Phys. Rev. Lett. **116**, 066401 (2016).
- [59] M. P. A. Fisher, P. B. Weichman, G. Grinstein, and D. S. Fisher, Physical Review B **40**, 546 (1989).
- [60] J. V. Jose, L. P. Kadanoff, S. Kirkpatrick, and D. R. Nelson, Physical Review B **16**, 1217 (1977).

SUPPLEMENTAL MATERIALS FOR ‘FATE OF A MULTIPLE-BAND FERMION LIQUID THAT IS COUPLED WITH CRITICAL ϕ^4 BOSONS’

ACTION FOR A FERMION-BOSON COUPLED SYSTEM

A two-bands fermion system coupled with a scalar boson field is considered. The fermion-boson coupling is given by the Yukawa coupling. An action for the scalar boson field is described by the $(d+1)$ -dimensional ϕ^4 theory with the dynamical exponent $z = 1$. The fermion-boson coupled system is described by the following effective action,

$$S_t = S_\psi + S_\phi + S_{\psi-\phi}, \quad (17)$$

$$S_\psi = \sum_{\sigma=\pm} \int \psi_\sigma^\dagger(\mathbf{x}, \tau) [\partial_\tau + \mu - E_\sigma(i\nabla)] \psi_\sigma(\mathbf{x}, \tau), \quad (18)$$

$$S_\phi = \int [m_0^2 |\phi|^2 + |\partial_\tau \phi|^2 + c_0^2 |\nabla \phi|^2 + \frac{\lambda_0}{4} (|\phi|^2)^2], \quad (19)$$

$$S_{\psi-\phi} = g_0 \int [\phi^\dagger \psi_+^\dagger \psi_- + \phi \psi_-^\dagger \psi_+], \quad (20)$$

$$\int \equiv \int d\tau \int d^d \mathbf{x}.$$

The coupled system has global U(1) symmetries;

$$\begin{cases} \text{(i)} & \psi_\pm^\dagger \rightarrow \psi_\pm^\dagger e^{\pm i\theta}, \quad \psi_\pm \rightarrow \psi_\pm e^{\mp i\theta}, \quad \phi^\dagger \rightarrow \phi^\dagger e^{-2i\theta} \\ \text{(ii)} & \psi_\pm^\dagger \rightarrow \psi_\pm^\dagger e^{i\theta}, \quad \psi_\pm \rightarrow \psi_\pm e^{-i\theta}. \end{cases} \quad (21)$$

The kinetic energy of the free fermion part is isotropic in the d -dimensional space, and an momentum-energy dispersion for the two fermion bands depend only on a norm of momentum, $E_\sigma(|\mathbf{k}|)$ ($\sigma = \pm$). In the paper, the two fermion's energy bands are an electron-type

band ($\sigma = +$) and hole-type band ($\sigma = -$) respectively. The chemical potential for the fermions is fine-tuned to a charge neutrality point (CNP), where the isotropic Fermi surface of the electron and that of the hole become identical to each other.

The two momentum-energy dispersions are linearized around the isotropic Fermi surface. The fermion part is described by a free theory with the dynamical exponent $z = 1$;

$$\begin{aligned} S_\psi &= \int \frac{d^{d+1}k}{(2\pi)^{d+1}} \psi_+^\dagger(k) [i\omega - v_{+0}l] \psi_+(k) \\ &\quad + \int \frac{d^{d+1}k}{(2\pi)^{d+1}} \psi_-^\dagger(k) [i\omega + v_{-0}l] \psi_-(k), \\ &\equiv \sum_{\sigma=\pm} \int_{\Omega, \omega, l} \psi_\sigma^\dagger(k) [i\omega - \sigma v_{\sigma 0}l] \psi_\sigma(k), \end{aligned} \quad (22)$$

and

$$\int_k \equiv k_F^{d-1} \int \frac{d^{d-1}\hat{\Omega}}{(2\pi)^{d-1}} \int_{-\bar{\Lambda}_F}^{\bar{\Lambda}_F} \frac{d\omega}{2\pi} \int_{-\Lambda_F}^{\Lambda_F} \frac{dl}{2\pi}, \quad (23)$$

with $v_{+0} > 0$, $v_{-0} > 0$, $k \equiv (\omega, \mathbf{k})$ and $\mathbf{k} = (k_F + l)\hat{\Omega}$. k_F is the Fermi wavelength of the isotropic Fermi surface and l is the perpendicular component of the d -dimensional momentum, and $\hat{\Omega}$ is a unit vector in the d -dimensional momentum space. In the presence of the isotropic Fermi surface, the d -dimensional momentum integral is decomposed into one-dimensional integral over l and $(d-1)$ -dimensional integral over $\hat{\Omega}$. Λ_F and $\bar{\Lambda}_F$ are high energy (ultraviolet) cutoff for the one-dimensional l -integral and the frequency (ω) integral respectively.

The boson part and the coupling part of the action are given in the momentum-frequency space,

$$\begin{aligned} S_\phi &= \int_q (m_0^2 + c_0^2 q^2 + \varepsilon^2) \phi^\dagger(q) \phi(q) \\ &\quad + \frac{\lambda_0}{4} \int_{q_1, q_2, q_3} (\phi^\dagger(q_1) \phi(q_2)) (\phi^\dagger(q_3) \phi(q_1 + q_3 - q_2)), \end{aligned} \quad (24)$$

$$S_{\psi-\phi} = g_0 \int_{k, q} [\phi^\dagger(q) \psi_+^\dagger(k) \psi_-(k+q) + \text{h.c.}], \quad (25)$$

with $q \equiv (\varepsilon, \mathbf{q})$, $q_j \equiv (\varepsilon_j, \mathbf{q}_j)$ ($j = 1, 2, \dots$), and

$$\int_q \equiv \int_{|\mathbf{q}| < \Lambda_B} \frac{d^d \mathbf{q}}{(2\pi)^d} \int_{-\bar{\Lambda}_B}^{\bar{\Lambda}_B} \frac{d\varepsilon}{2\pi}, \quad (26)$$

$$\int_{k, q} \equiv \int_k \int_q, \quad \int_{q_1, q_2, q_3} \equiv \int_{q_1} \int_{q_2} \int_{q_3}. \quad (27)$$

Here Λ_B and $\bar{\Lambda}_B$ are the ultraviolet (UV) cutoff for the boson momentum and frequency.

The vertex and Green's functions play the central role in the paper. Let us call as $\Gamma^{(N_F, N_B)}$ and $G^{(N_F, N_B)}$ the vertex and Green's function respectively, that have N_F

external fermion lines and N_B external boson lines. The Green functions are introduced together with the effective action S_t as,

$$\begin{aligned}
(2\pi)^{d+1}\delta^{d+1}(k-k')\delta_{\sigma,\sigma'}G_{\sigma}^{(2,0)}(k) &\equiv \langle \psi_{\sigma}(k)\psi_{\sigma'}^{\dagger}(k') \rangle, \\
(2\pi)^{d+1}\delta^{d+1}(q-q')G^{(0,2)}(q) &\equiv \langle \phi(q)\phi^{\dagger}(q') \rangle, \\
(2\pi)^{d+1}\delta^{d+1}(k'-k-q)G_{+}^{(2,1)}(k,k+q;q) \\
&\equiv \langle \psi_{+}(k)\psi_{-}^{\dagger}(k')\phi(q) \rangle, \\
(2\pi)^{d+1}\delta^{d+1}(k'-k+q)G_{-}^{(2,1)}(k,k-q;q) \\
&\equiv \langle \psi_{-}(k)\psi_{+}^{\dagger}(k')\phi^{\dagger}(q) \rangle, \\
(2\pi)^{d+1}\delta^{d+1}(q_4+q_3-q_2-q_1)G^{(0,4)}(q_1,q_2,q_3) \\
&\equiv \langle \phi(q_4)\phi(q_3)\phi^{\dagger}(q_2)\phi^{\dagger}(q_1) \rangle, \quad (28)
\end{aligned}$$

and

$$\begin{aligned}
\langle \dots \rangle &\equiv \frac{1}{Z} \int D\phi^{\dagger} D\phi D\psi^{\dagger} D\psi e^{-S_t} \dots, \\
Z &\equiv \int D\phi^{\dagger} D\phi D\psi^{\dagger} D\psi e^{-S_t}. \quad (29)
\end{aligned}$$

Here the band index $\sigma, \sigma' = \pm$ in Eq. (28) is an additional subscript, that distinguishes different functions for same N_F and N_B . Because of the U(1) gauge symmetry Eq. (21), $G^{(2,1)}$ has only two different functions; $G_{\pm}^{(2,1)}$. $G^{(0,4)}$ comprises of connected and disconnected parts. The disconnected part is given by products of two $G^{(0,2)}$. The vertex functions are obtained from an amputation of the one-particle irreducible (1PI) parts of the connected Green's functions;

$$\begin{aligned}
G_{\sigma}^{(2,0)}(k)\Gamma_{\sigma}^{(2,0)}(k) &\equiv 1, \quad G^{(0,2)}(q)\Gamma^{(0,2)}(q) \equiv 1, \\
G_{\pm}^{(2,1)}(k,k \pm q;q) &\equiv \\
&G_{\pm}^{(2,0)}(k)G_{\mp}^{(2,0)}(k \pm q)G^{(0,2)}(q)\Gamma_{\pm}^{(2,1)}(k,k \pm q;q), \\
G^{(0,4)}(q_1,q_2,q_3) &\equiv G^{(0,2)}(q_1)G^{(0,2)}(q_2)G^{(0,2)}(q_3) \\
&\times G^{(0,2)}(q_1+q_2-q_3)\Gamma^{(0,4)}(q_1,q_2,q_3) + \dots \quad (30)
\end{aligned}$$

Here ' \dots ' in the last line stands for the disconnected part of $G^{(0,4)}$.

For the effective model of Eqs. (22,24,25), the vertex function $\Gamma^{(N_F, N_B)}$ has potentially an ultraviolet (UV) divergence in the power of a large UV cutoff Λ , which is either Λ_B , $\bar{\Lambda}_B$, Λ_F or $\bar{\Lambda}_F$ defined in Eqs. (23,26,27). The degree of the UV divergence depends on the number of the external lines, N_F and N_B , and the spatial dimension d . By the field theory, $\Gamma^{(N_F, N_B)}$ is given by a sum of amputated Feynman diagrams for the 1PI connected $G^{(N_F, N_B)}$. Each amputated Feynman diagram is given by an integral over L -number of internal D -dimensional momenta (frequency and momentum) with $D \equiv d+1$. The integrand is a product among V_F -number of internal fermion lines (fermion Green's functions), V_B internal boson lines (boson Green's functions), V_1 vertices of the

Yukawa couplings (g_0) and V_2 vertices of the ϕ^4 coupling (λ_0). Such an integral can have a UV divergence with respect to the large UV cutoff Λ . The degree of the divergence can be superficially evaluated by a dimensional counting of the integral [53, 54]. From the dimensional counting, the superficial degree of the UV divergence, M , is bounded from above by $D_{\max} = DL - V_F - 2V_B$; $M \leq D_{\max}$. Here the equality holds true for those amputated Feynman diagrams which do not have any integrals over internal fermion momenta. The inequality applies for those Feynman diagrams which have the integrals over the internal fermion momenta (see also below). A sum of the internal and external boson lines in the connected $G^{(N_F, N_B)}$ is given by $V_1/2 + 2V_2 + N_B/2 \equiv V_B + N_B$, while a sum of the internal and external fermion lines is by $V_1 + N_F/2 \equiv V_F + N_F$. In terms of these two identities together with $L = V_F + V_B - V_1 - V_2 + 1$, the dependences on V_F and V_B in D_{\max} and L can be eliminated,

$$\begin{aligned}
D_{\max} = D + \frac{D-4}{2}V_1 + (D-4)V_2 \\
- \frac{D-1}{2}N_F - \frac{D-2}{2}N_B, \quad (31)
\end{aligned}$$

and

$$L = \frac{V_1}{2} + V_2 - \frac{N_F}{2} - \frac{N_B}{2} + 1. \quad (32)$$

Eq. (31) suggests that $D = 4$ ($d = 3$) is an upper critical dimension, where the effective model of Eqs. (22,24,25) is renormalizable. Eq. (32) shows that for fixed N_E and N_B , the number of the internal integral variables L increases with a unit of either $V_1 = 2$ or $V_2 = 1$.

The paper focuses on the upper critical dimension of the effective model, where only the following four vertex functions have potentially the UV divergences at $D = 4$,

$$\Gamma^{(2,0)}, \Gamma^{(0,2)}, \Gamma^{(2,1)}, \Gamma^{(0,4)}. \quad (33)$$

From Eq. (31), their superficial degrees of the UV divergences in the power of the UV cutoff Λ are evaluated (at most) 1, 2, 0 and 0 respectively. Note that both $\Gamma^{(1,0)}$, $\Gamma^{(0,1)}$ and $\Gamma^{(1,1)}$ are zero because of the gauge symmetries; Eq. (21). In the next section, we will use a renormalized perturbation theory and eliminate the dependences of the UV cutoff from these vertex functions by way of renormalizations of field operator amplitudes, boson mass, fermion velocities, boson velocity, Yukawa coupling and the ϕ^4 coupling.

Before closing this section, let us explain how the Fermi wavelength k_F is treated in the paper. The effective model implicitly assumes that the Fermi wavelength k_F is much larger than the UV cutoff Λ and the UV cutoff is much larger than fermion and boson momenta in Eqs. (22,24,25);

$$|q|, \varepsilon, \omega, l \ll \Lambda_B, \bar{\Lambda}_B, \Lambda_F, \bar{\Lambda}_F \ll k_F. \quad (34)$$

The renormalized theory shall be free from the UV cutoff Λ (being Λ_B , $\bar{\Lambda}_B$, Λ_F or $\bar{\Lambda}_F$), where $|\mathbf{q}|/\Lambda$, ε/Λ , l/Λ , ω/Λ are regarded as infinitesimally small and set to zero in the renormalized vertex functions. Meanwhile, we will allow the renormalized functions to depend not only on the boson and fermion momenta \mathbf{q} , ε , ω , l but also on the Fermi wavelength k_F . That says, the Fermi wavelength is treated as a finite (although the largest) measurable physical quantity.

To enable such an exceptional treatment of k_F in spite of $|\mathbf{q}|$, ε , ω , $l \ll \Lambda \ll k_F$, it is important to note that all the vertex functions in Eq. (33) can be expanded in the power of k_F^{d-1} ;

$$\Gamma^{(N_F, N_B)} = \Gamma^{(N_F, N_B; 0)} + k_F^{d-1} \Gamma^{(N_F, N_B; 1)} + k_F^{2(d-1)} \Gamma^{(N_F, N_B; 2)} + \dots, \quad (N_F = 0, 2). \quad (35)$$

Here $k_F^{n(d-1)} \Gamma^{(N_F, N_B; n)}$ in the right hand side is a sum of all those amputated 1PI Feynman diagrams for $\Gamma^{(N_F, N_B)}$ that have n numbers of internal closed loops formed by fermion lines ('closed fermion loops'). Importantly, *it has no k_F -dependence other than the overall factor, $k_F^{n(d-1)}$, for $N_F = 0, 2$* . To see this, let us consider how to assign the L -number of the internal integral variables to the $(V_F + V_B)$ -number of the internal lines in an ampu-

tated 1PI Feynman diagram with n -number of the closed fermion loops. The most natural way of doing this in the case of $\Lambda \ll k_F$ is as follows. For each closed fermion loop, say the j -th closed fermion loop with $j = 1, \dots, n$, assign an integral variable of fermion momentum to one and *only* one internal fermion line in the loop, say (ω_j, \mathbf{k}_j) with $\mathbf{k}_j = (k_F + l_j)\hat{\Omega}_j$. Meanwhile, assign the other $(L - n)$ -number of the integral variables to the internal boson lines, such that momentum and frequency conservations are preserved at every vertex. The momenta of the other internal fermion lines in the j -th closed fermion loop shall be given by a sum of (ω_j, \mathbf{k}_j) and the boson momenta (either internal or external). For $N_F = 2$ with an open fermion line with two external fermion points, one of the two external fermions is given by (ω, \mathbf{k}) , while the other external fermion is given by a sum of (ω, \mathbf{k}) and external boson momenta (if any). Thereby, the momenta of the internal fermions in the open fermion line shall be given by a sum of the external fermion momentum (ω, \mathbf{k}) and (either internal or external) boson momenta. With this way of the assignment of the integral variables, the integrand clearly has no k_F -dependence in the case of $\Lambda \ll k_F$. The only k_F -dependence in the integral appears through the overall factor, $k_F^{n(d-1)}$;

$$k_F^{n(d-1)} \Gamma^{(N_F \leq 2, N_B; n)} = k_F^{n(d-1)} \sum_L \int \frac{d^{d-1} \hat{\Omega}_1}{(2\pi)^{d-1}} \int_{\Lambda} \frac{d\omega_1 dl_1}{(2\pi)^2} \dots \int \frac{d^{d-1} \hat{\Omega}_n}{(2\pi)^{d-1}} \int_{\Lambda} \frac{d\omega_n dl_n}{(2\pi)^2} \int_{\Lambda} \frac{d^{d+1} q_1}{(2\pi)^{d+1}} \dots \int_{\Lambda} \frac{d^{d+1} q_{L-n}}{(2\pi)^{d+1}} (\text{integrand that is free from } k_F). \quad (36)$$

In $\Gamma^{(N_F, N_B; n)}$ thus given, the superficial degree of the UV divergence with respect to the power in Λ is smaller than that of $\Gamma^{(N_F, N_B; 0)}$ by $n(d-1)$.

$$\begin{cases} \left[\Gamma^{(N_F, N_B; 0)} \right] = DL - V_F - 2V_B \equiv D_{\max}, \\ \left[\Gamma^{(N_F, N_B; 1)} \right] = D_{\max} - (d-1), \\ \left[\Gamma^{(N_F, N_B; 2)} \right] = D_{\max} - 2(d-1), \quad \dots, \\ \left[\Gamma^{(N_F, N_B; n)} \right] = D_{\max} - n(d-1), \quad \dots \end{cases} \quad (37)$$

The integer in the right hand side refers to the superficial degree of the UV divergence in the left hand side. When the integer in the right hand side is less than 0, the left hand side should be regarded as on the order of $\mathcal{O}(1)$ in the power of the UV cutoff Λ .

Thanks to the analytic feature of the vertex functions as functions of k_F , Eq. (35), the dependence on the UV cutoff Λ in the vertex functions can be removed at every order in k_F^{d-1} . Generally speaking, higher orders in k_F^{d-1} mean smaller numbers of the superficial degree of the UV divergences in Λ ; Eq. (37). Thus, it is usually the case

that only a few low-order powers in k_F^{d-1} need to be considered in the expansion. In the paper, we consider $d = 3$ and carry out the renormalizations of the zeroth order of $\Gamma^{(2,0)}$ whose UV divergence degree in Λ is 1 (Sec. IIIA), and the zeroth and first order of $\Gamma^{(0,2)}$ whose UV divergence degrees in Λ are 2 and 0 respectively (Sec. IIIB). To this end, renormalization conditions for the vertex functions will be expanded in the powers of k_F^2 ($d = 3$). See Eq. (45), where a renormalization condition on the boson self-energy part is given up to the first order in k_F^2 . A dimensional analysis suggests that renormalized $\Gamma^{(N_F, N_B; n)}$ thus obtained has a different scaling form for different n ; see Eq. (113) for example. In each of these scaling forms, the boson and fermion momenta, q , ε , ω , l , must be treated as much smaller than k_F ; Eq. (34). In Sec. III, asymptotic behaviours of the boson and fermion spectral functions will be clarified for such small momentum and frequency region. It turns out that the asymptotic behaviours with respect to the small momenta are

free from k_F , while overall factors of the spectral weights can have an explicit dependence on k_F (Sec. IIIB).

RENORMALIZATION

In this section, we will eliminate the UV divergences in all the vertex functions in Eq. (33), while include the UV cutoff dependences into the renormalizations of the field operator amplitudes and physical quantities. To see how many physical quantities are needed for this purpose, let us first expand their superficial degrees of the UV divergence in terms of the external momentum and frequency,

$$\begin{aligned}\Gamma_{\sigma}^{(2,0)}(i\omega, \mathbf{k}) &= \dots \Lambda + \dots \ln \Lambda i\omega + \dots \ln \Lambda l, \\ \Gamma_{\sigma}^{(0,2)}(i\varepsilon, \mathbf{q}) &= \dots \Lambda^2 + \dots \ln \Lambda \varepsilon^2 + \dots \ln \Lambda \mathbf{q}^2, \\ \Gamma_{\sigma}^{(2,1)}(\dots) &= \dots \ln \Lambda + \mathcal{O}(\omega, l, q), \\ \Gamma_{\sigma}^{(0,4)}(\dots) &= \dots \ln \Lambda + \mathcal{O}(\omega, l, q),\end{aligned}$$

with $\sigma = \pm$ and $\mathbf{k} = (k_F + l)\hat{\Omega}$. Here the UV cutoff Λ is either Λ_F , $\bar{\Lambda}_F$, Λ_B or $\bar{\Lambda}_B$. For each of the two fermion bands ($\sigma = \pm$), $\Gamma_{\sigma}^{(2,0)}(i\omega, \mathbf{k})$ has a linear divergence in Λ , that corresponds to an energy shift of each fermion energy band. $\Gamma_{\sigma}^{(2,0)}(i\omega, \mathbf{k})$ also has the logarithmic UV divergences in its linear terms of its frequency ω and the one-dimensional momentum l . These logarithmic divergences correspond to the renormalizations of the fermion field operator amplitude and the Fermi velocity respectively. The two-point boson vertex function has the logarithmic divergences in the quadratic terms of its frequency and momentum. They correspond to the renormalizations of the boson field operator amplitude and boson velocity. In total, the theory in $d = 3$ ($D = 4$) has eleven kinds of the UV divergences with respect to the UV cutoff Λ . To renormalize all of them, one should use the shifts of the Fermi wavelengths, $\delta k_{F\sigma}$ ($\sigma = \pm$), renormalizations of the fermion field amplitudes, Z_{σ} ($\sigma = \pm$), the fermion velocities, v_{σ} ($\sigma = \pm$), the boson field amplitude, Z_{ϕ} , boson mass, m^2 , boson velocity, c^2 , the Yukawa coupling g and the ϕ^4 coupling λ . As shown below (Sec. IIC), the Λ -linear terms in $\Gamma_{\pm}^{(2,0)}$ do not appear in the following perturbation theory calculation; $\delta k_{F\sigma} = 0$. We thus consider only the renormalizations of Z_{σ} , v_{σ} ($\sigma = \pm$), Z_{ϕ} , m^2 , c^2 , g and λ , while taking the Fermi wavelength to be always k_F ; $k_{F\sigma} = k_{F0} + \delta k_{F\sigma} \equiv k_F$ ($\sigma = \pm$, k_{F0} is a bare Fermi wavelength).

renormalized Green's and vertex functions, effective action and counterterms part

Based on this observation, we employ the minimal subtraction scheme [53, 54], and decompose the bare action

S_t into the effective action S_E and counterterms part S_c ,

$$\begin{aligned}S_t &= S_E + S_c \\ S_E &= \sum_{\sigma=\pm} \int_{\Omega, \omega, l} \bar{\psi}_{\sigma}^{\dagger}(k) [i\omega - \sigma v_{\sigma} l] \bar{\psi}_{\sigma}(k) \\ &\quad + \int_q (m^2 + c^2 \mathbf{q}^2 + \varepsilon^2) \bar{\phi}^{\dagger}(q) \bar{\phi}(q) \\ &\quad + \frac{\lambda}{4} \int_{q_1, q_2, q_3} (\bar{\phi}^{\dagger}(q_1) \bar{\phi}(q_2)) (\bar{\phi}^{\dagger}(q_3) \bar{\phi}(q_1 + q_3 - q_2)) \\ &\quad + g \int_{k, q} [\bar{\phi}^{\dagger}(q) \bar{\psi}_{+}^{\dagger}(k) \bar{\psi}_{-}(k + q) + \text{c.c.}] \\ S_c &= \sum_{\sigma} \int_{\Omega, \omega, l} \bar{\psi}_{\sigma}^{\dagger} [i\delta_{\sigma} \omega - \sigma \delta v_{\sigma} l] \bar{\psi}_{\sigma} \\ &\quad + \int_q (\delta m^2 + \delta c^2 \mathbf{q}^2 + \delta_{\phi} \varepsilon^2) \bar{\phi}^{\dagger} \bar{\phi} \\ &\quad + \frac{\delta \lambda}{4} \int_{q_1, q_2, q_3} (\bar{\phi}^{\dagger} \bar{\phi}) (\bar{\phi}^{\dagger} \bar{\phi}) + \delta g \int_{k, q} [\bar{\phi}^{\dagger} \bar{\psi}_{+}^{\dagger} \bar{\psi}_{-} + \text{c.c.}].\end{aligned}\tag{38}$$

Here renormalized field operators ($\bar{\psi}_{+}$, $\bar{\psi}_{-}$, $\bar{\phi}$) and renormalized physical quantities (c^2 , v_{+} , v_{-} , m^2 , g , λ) are related with their bare and counterparts by,

$$\begin{aligned}\psi_{\sigma} &\equiv \sqrt{Z_{\sigma}} \bar{\psi}_{\sigma}, \phi \equiv \sqrt{Z_{\phi}} \bar{\phi}, c_0^2 \equiv Z_{c^2} c^2, v_{\sigma 0} \equiv Z_{v_{\sigma}} v_{\sigma}, \\ m_0^2 &\equiv Z_m m^2, g_0 \equiv \frac{Z_g}{\sqrt{Z_{\phi} Z_{+} Z_{-}}} g, \lambda_0 \equiv \frac{Z_{\lambda}}{Z_{\phi}^2} \lambda,\end{aligned}\tag{40}$$

and

$$\begin{aligned}Z_{\sigma} &\equiv 1 + \delta_{\sigma}, Z_{\phi} \equiv 1 + \delta_{\phi}, Z_{\sigma} Z_{v_{\sigma}} v_{\sigma} \equiv v_{\sigma} + \delta v_{\sigma}, \\ Z_{\phi} Z_{c^2} c^2 &\equiv c^2 + \delta c^2, Z_{\phi} Z_m m^2 \equiv m^2 + \delta m^2, \\ Z_g g &\equiv g + \delta g, Z_{\lambda} \lambda \equiv \lambda + \delta \lambda.\end{aligned}\tag{41}$$

with $\sigma = \pm$.

The objective of the renormalization theory is to include all the UV divergences in the bare vertex functions into the renormalizations of the field operator amplitudes (Z_{\pm} , Z_{ϕ}) and bare quantities ($v_{\pm 0}$, c_0^2 , m_0 , g_0 , λ_0), while making renormalized vertex functions and renormalized physical quantities (v_{\pm} , c^2 , m , g , λ) to be free from the UV cutoff. Thereby, the renormalized Green's and vertex functions are defined in the same way as Eqs. (28,30)

with ψ_{\pm} and ϕ being replaced by $\bar{\psi}_{\pm}$ and $\bar{\phi}$, e.g.

$$\begin{aligned}
(2\pi)^4 \delta^4(k - k') \delta_{\sigma, \sigma'} \bar{G}_{\sigma}^{(2,0)}(k) &\equiv \langle \bar{\psi}_{\sigma}(k) \bar{\psi}_{\sigma'}^{\dagger}(k') \rangle, \\
(2\pi)^4 \delta^4(q - q') \bar{G}^{(0,2)}(q) &\equiv \langle \bar{\phi}(q) \bar{\phi}^{\dagger}(q') \rangle, \\
\bar{G}_{\sigma}^{(2,0)}(k) \bar{\Gamma}_{\sigma}^{(2,0)}(k) &= 1, \quad \bar{G}^{(0,2)}(q) \bar{\Gamma}^{(0,2)}(q) = 1, \\
(2\pi)^4 \delta^4(k' - k - q) \bar{G}_{+}^{(2,1)}(k, k + q; q) &\equiv \langle \bar{\psi}_{+}(k) \bar{\psi}_{-}^{\dagger}(k') \bar{\phi}(q) \rangle \\
&= \bar{G}_{+}^{(2,0)}(k) \bar{G}_{-}^{(2,0)}(k + q) \bar{G}^{(0,2)}(q) \bar{\Gamma}_{+}^{(2,1)}(k, k + q; q), \\
(2\pi)^4 \delta^4(q_4 + q_3 - q_2 - q_1) \bar{G}^{(0,4)}(q_1, q_2, q_3) \\
&\equiv \langle \bar{\phi}(q_4) \bar{\phi}(q_3) \bar{\phi}^{\dagger}(q_2) \bar{\phi}^{\dagger}(q_1) \rangle, \\
\bar{G}^{(0,4)}(q_1, q_2, q_3) &= \bar{G}^{(0,2)}(q_1) \bar{G}^{(0,2)}(q_2) \bar{G}^{(0,2)}(q_3) \\
&\times \bar{G}^{(0,2)}(q_1 + q_2 - q_3) \bar{\Gamma}^{(0,4)}(q_1, q_2, q_3) + \dots \quad (42)
\end{aligned}$$

Note that $\langle \dots \rangle$ in the right hand sides is defined in Eq. (29) with the same S_t as in Eq. (17) with $d = 3$. Thus, the renormalized Green's and vertex functions dif-

fer from their bare functions only by Z_{ϕ} and/or Z_{\pm} ,

$$\begin{aligned}
G_{\sigma}^{(2,0)}(k) &= Z_{\sigma} \bar{G}_{\sigma}^{(2,0)}(k), \quad G^{(0,2)}(q) = Z_{\phi} \bar{G}^{(0,2)}(q), \\
\bar{\Gamma}^{(2,1)}(k, k + q; q) &= Z_{+}^{\frac{1}{2}} Z_{-}^{\frac{1}{2}} Z_{\phi}^{\frac{1}{2}} \bar{\Gamma}^{(2,1)}(k, k + q; q), \\
\bar{\Gamma}^{(0,4)}(q_1, q_2, q_3) &= Z_{\phi}^2 \bar{\Gamma}^{(0,4)}(q_1, q_2, q_3). \quad (43)
\end{aligned}$$

In the following, we will omit the superscripts of (N_F, N_B) from the Green's and vertex functions and use the following simplified notations,

$$\begin{aligned}
\bar{G}_{\sigma}^{(2,0)} &\rightarrow \bar{G}_{\sigma}, \quad \bar{G}^{(0,2)} \rightarrow \bar{G}_{\phi}, \quad \bar{\Gamma}_{\sigma}^{(2,0)} \rightarrow \bar{G}_{\sigma}^{-1}, \\
\bar{\Gamma}^{(0,2)} &\rightarrow \bar{G}_{\phi}^{-1}, \quad \bar{\Gamma}_{+}^{(2,1)} \rightarrow \bar{\Gamma}_g, \quad \bar{\Gamma}^{(0,4)} \rightarrow \bar{\Gamma}_{\lambda}, \quad (44)
\end{aligned}$$

with $\sigma = \pm$.

renormalization conditions

To make the renormalized vertex functions to be free from the UV cutoff Λ , we impose the following conditions on the vertex functions,

$$\begin{cases} \bar{G}_{\sigma}^{-1}(\omega = l = 0) = 0, \quad \frac{\partial \bar{G}_{\sigma}^{-1}(\omega, l)}{\partial(i\omega)} \Big|_{v_{\sigma} l = 0, \omega = K} = 1 \quad (\sigma = \pm), \quad \frac{\partial \bar{G}_{\sigma}^{-1}(\omega, l)}{\partial(-v_{\sigma} l)} \Big|_{v_{\sigma} l = K, \omega = 0} = \frac{\partial \bar{G}_{\sigma}^{-1}(\omega, l)}{\partial(v_{\sigma} l)} \Big|_{v_{\sigma} l = K, \omega = 0} = 1 \\ \bar{G}_{\phi}^{-1}(\varepsilon = Q, |\mathbf{q}| = 0) = m^2 + Q^2, \quad \frac{\partial \bar{G}_{\phi}^{-1}(q)}{\partial \varepsilon} \Big|_{\mathbf{q}=0, \varepsilon=Q} = \frac{\partial \bar{G}_{\phi}^{-1}(q)}{\partial(c|\mathbf{q}|)} \Big|_{c|\mathbf{q}|=Q, \varepsilon=0} = 2Q + \frac{g^2}{\pi^2(v_{+} + v_{-})} \frac{k_F^2}{Q}, \\ \bar{\Gamma}_g(k, k + q; q) \Big|_{q=0, \omega=l=0} = -g, \quad \bar{\Gamma}_{\lambda}(q_1, q_2, q_3) \Big|_{q_1=(P,0), q_2=(P/3,0), q_3=(2P/3,0)} = -\lambda, \end{cases} \quad (45)$$

with $k = (\omega, \mathbf{k})$, $\mathbf{k} = (k_F + l)\hat{\Omega}$, and $q = (\varepsilon, \mathbf{q})$. Importantly, the right hand sides of the conditions are free from the UV cutoff Λ . They depend only on physical quantities such as the Fermi wavelength k_F , renormalized boson mass, m , renormalized velocities, v_{\pm} , c , and renormalized coupling constants, g , λ .

A 1-loop proper part of the fermion self energy has a weak infrared (IR) singularity (Fig. 4(a); $\omega \log \omega$ in small external frequency ω or l ; see Sec. IIC). Thus, the condition on its derivatives is imposed at finite ω or $v_{\pm} l = K$. A 1-loop proper part of the boson self-energy has an IR logarithmic divergence, that comes from the fermion's polarization function (Fig. 4(b); see Sec. IID). The polarization function has a closed fermion loop, so that it is proportional to k_F^2 . When being taken a derivative of with respect to q , the IR logarithmic divergence leads to a IR linear divergence. To circumvent these IR divergences, we set the external boson frequency and momentum at finite value, ε or $c|\mathbf{q}| = Q$. Besides, we expand in the power of k_F^2 the right hand side of the condition for the derivatives of the boson self-energy. The zeroth order in the expansion would take care of the usual

logarithmic UV divergence in the quadratic terms of the external boson momenta, that come from 2-loop corrections. The first order in the expansion is for canceling the IR linear divergence from the fermion's polarization function. See Eq. (35) and text around this equation for an explanation of the k_F^2 -expansion.

A 1-loop four-point boson vertex function can have an IR quadratic divergence, depending on its four external boson momenta (Fig. 4(e)). The IR quadratic divergence comes from an integral over an internal fermion momentum and frequency. We choose the external boson frequencies, in such a way that the one-loop integral over the fermion momentum becomes zero (See Sec. IIE);

$$\begin{aligned}
q_1 &\equiv (\varepsilon_1, \mathbf{q}_1) = (P, \mathbf{0}), \quad q_2 = (P/3, \mathbf{0}), \\
q_3 &= (2P/3, \mathbf{0}), \quad q_4 = (2P/3, \mathbf{0}). \quad (46)
\end{aligned}$$

For the other choice of the external boson frequencies, the one-loop integral has an IR quadratic divergence and in that case, we could modify the conditions. Namely, we could expand in the power of k_F^2 the right hand side of the condition for the four-point boson vertex function, and add the first order term in k_F^2 , that cancels the IR

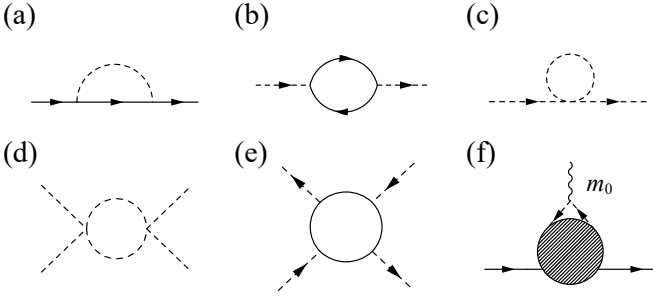


FIG. 4. (a-e) One-loop Feynman diagrams included in the renormalized perturbation analysis. (f) $\Gamma^{(2,2)}(k, k; q, q)$. The solid/broken line is fermion/boson line respectively. A wavy line represents a boson mass m_0 , that comes with a pair of boson lines.

quadratic divergent term.

Q , K and P in Eq. (45) are external frequencies or momenta, at which the renormalization conditions are imposed on the 2-point fermion, 2-point boson and 4-point boson vertex functions respectively. When these three energy scales were treated as three independent renormalization group (RG) scale variables, a β function of the same physical quantity would depend on the type of the vertex function, for which a Callan-Symanzik (CS) equation with the β function would be solved. Such is against our intuition of universality in critical phenomena. We thus set Q , K and P as the *same* RG scale variable κ ,

$$Q = K = P \equiv \kappa. \quad (47)$$

The renormalization conditions in Eq. (45) eliminate all the UV divergences in the renormalized vertex functions, while the UV dependences are put into the renormalizations of the field operator amplitudes (Z_{\pm} , Z_{ϕ}), and bare quantities (m_0^2 , v_{+0} , v_{-0} , c_0^2 , g_0 , λ_0).

In terms of the renormalized perturbation theory, the renormalization conditions shall be satisfied perturbatively in the (renormalized) Yukawa coupling g and the ϕ^4 coupling λ . To this end, we treat as perturbations g and λ in S_E as well as the counterterms S_c and treat the quadratic part in S_E as the free part. Eq. (32) shows that for fixed N_F and N_B , the number of the internal integral variables (L) increases with a unit of g^2 or λ . We thus treat g^2 and λ as the same order of the smallness in the perturbation analysis. The standard Dyson-Feynman perturbation theory leads to following one-loop terms ($L = 1$) for the amputated 1PI connected Green's

functions (Fig. 4(a-e)),

$$\begin{aligned} \bar{G}_{\pm}^{-1}(k) &= \bar{G}_{\pm,0}^{-1}(k) + (\delta_{\pm} i\omega \mp \delta v_{\pm} l) \\ &\quad - g^2 \int_q \bar{G}_{\mp,0}(k+q) \bar{G}_{\phi,0}(q) + \mathcal{O}(g^4, g^2 \lambda, \lambda^2), \end{aligned} \quad (48)$$

$$\begin{aligned} \bar{G}_{\phi}^{-1}(q) &= \bar{G}_{\phi,0}^{-1}(q) + (\delta m^2 + \delta c^2 q^2 + \delta_{\phi} \varepsilon^2) \\ &\quad + g^2 \int_k \bar{G}_{+,0}(k+q) \bar{G}_{-,0}(k) + \lambda \int_{q'} \bar{G}_{\phi,0}(q') \\ &\quad + \mathcal{O}(g^4, g^2 \lambda, \lambda^2), \end{aligned} \quad (49)$$

$$\bar{\Gamma}_g(k, k+q; q) = -g - \delta g + \mathcal{O}(g^5, g^3 \lambda, g \lambda^2), \quad (50)$$

$$\begin{aligned} \bar{\Gamma}_{\lambda}(q_1, q_2, q_3) &= -\lambda - \delta \lambda + \frac{\lambda^2}{2} \int_q \bar{G}_{\phi,0}(q) \bar{G}_{\phi,0}(q_1 + q_2 - q) \\ &\quad + \lambda^2 \int_q \bar{G}_{\phi,0}(q) \left(\bar{G}_{\phi,0}(q + q_2 - q_3) + \bar{G}_{\phi,0}(q + q_1 - q_3) \right) \\ &\quad - g^4 \int_k \bar{G}_{+,0}(k) \bar{G}_{-,0}(k + q_1) \left(\bar{G}_{+,0}(k + q_1 - q_3) \right. \\ &\quad \times \bar{G}_{-,0}(k + q_1 + q_2 - q_3) + \bar{G}_{+,0}(k - q_2 + q_3) \\ &\quad \times \bar{G}_{-,0}(k + q_3) \left. \right) + \mathcal{O}(\lambda^3, g^2 \lambda^2, g^4 \lambda, g^6), \end{aligned} \quad (51)$$

where renormalized free Green's functions for fermions and boson are given by

$$\bar{G}_{\pm,0}^{-1}(k) = i\omega \mp v_{\pm} l, \quad \bar{G}_{\phi,0}^{-1}(q) = m^2 + c^2 q^2 + \varepsilon^2, \quad (52)$$

with $q \equiv (\varepsilon, \mathbf{q})$, $k \equiv (\omega, \mathbf{k})$ and $\mathbf{k} = (k_F + l)\hat{\Omega}$. The integrals over q or k are defined in Eqs. (23,26,27). All the one-loop terms except for the last term in Eq. (51) have ultraviolet divergences. The last term in Eq. (51) has no influence on the β function for λ ; $\beta_{\lambda}(\dots)$. β_{λ} within the one-loop level is identical to that in the pure ϕ^4 theory. Note also that $\bar{\Gamma}_g(k, k+q; q)$ has no one-loop term because of the Yukawa coupling; $\sigma_{\pm} \sigma_{\pm} \sigma_{\mp} = 0$.

Calculation of $\int_q \bar{G}_{\mp,0}(k+q) \bar{G}_{\phi,0}(q)$ at $d = 3$

The 1-loop term in the fermion self-energy (Fig. 4(a)) has no linear divergence in Λ , while it has the logarithmic divergence in large Λ . To see this, we take Λ_B to the infinite in Eq. (26) and see how the integral depends on the UV cutoff for the boson momentum, Λ_B . Carry out first an integral over an angle between the internal boson

momentum and external fermion momentum,

$$\begin{aligned} \int_q \bar{G}_{+,0}(k+q) \bar{G}_{\phi,0}(q) &= \frac{1}{8\pi^3} \int_{-\infty}^{\infty} d\varepsilon \int_0^{\Lambda_B} Q^2 dQ \\ &\times \int_{-1}^1 dt \frac{1}{\varepsilon^2 + c^2 Q^2 + m^2} \frac{1}{i\omega - v_+ l + i\varepsilon - v_+ Q t} \\ &= -\frac{1}{8\pi^3 v_+} \int_0^{\Lambda_B} Q dQ \\ &\int_{-\infty}^{\infty} \frac{d\varepsilon}{(\varepsilon + iM)(\varepsilon - iM)} \text{Log} \left[\frac{i\omega + i\varepsilon - v_+ l - v_+ Q}{i\omega + i\varepsilon - v_+ l + v_+ Q} \right], \end{aligned} \quad (53)$$

with $q \equiv (i\varepsilon, \mathbf{q})$, $k \equiv (i\omega, \mathbf{k})$, $\mathbf{k} = (k_F + l)\hat{\Omega}$, $|\mathbf{q}| \equiv Q$, $Qt \equiv \mathbf{q} \cdot \hat{\Omega}$ and $M^2 \equiv c^2 Q^2 + m^2$. The integral is odd under $(\omega, l) \rightarrow -(\omega, l)$. Thus, without loss of generality, we can assume that l is positive. In the complex variable plane of ε , the integrand in the right hand side has a branch cut of the logarithmic function, which runs from $\varepsilon = -\omega - i v_+(l + Q)$ to $\varepsilon = -\omega - i v_+(l - Q)$. For $(0 <)Q < l$, the integral can be given by a pole contribution

at $\varepsilon = \pm iM$. For $l < Q$, The real axis of ε crosses the branch cut, so that the integral is composed of the pole contribution and an integral along the branch cut from $\varepsilon = -\omega$ to $\varepsilon = -\omega - i v_+(l \pm Q)$ respectively. This leads to

$$\begin{aligned} \int_q \bar{G}_{+,0}(k+q) \bar{G}_{\phi,0}(q) &= -\frac{1}{8\pi^2 v_+} \\ &\left(\int_0^l dQ \frac{Q}{M} \text{Log} \left[\frac{i\omega - M - v_+ l - v_+ Q}{i\omega - M - v_+ l + v_+ Q} \right] + \int_l^{\Lambda_B} dQ \frac{Q}{M} \right. \\ &\left. \left\{ \text{Log} \left[\frac{M + v_+ l + v_+ Q - i\omega}{M - v_+ l + v_+ Q + i\omega} \right] + \text{Log} \left[\frac{M + i\omega}{M - i\omega} \right] \right\} \right), \end{aligned} \quad (54)$$

for $l > 0$. At the massless point ($m = 0$), the integral over Q can be further carried out explicitly. Besides, replacing v_+ by $-v_-$ in Eq. (53) is equivalent to changing ω by $-\omega$ and adding the overall minus sign in Eq. (53). This leads to

$$\begin{aligned} \int_q \bar{G}_{\sigma,0}(k+q) \bar{G}_{\phi,0}(q) \Big|_{m=0} &= -\frac{\sigma}{8\pi^2 c v_\sigma} \left\{ -\left(\frac{1}{c + v_\sigma} - \frac{1}{c - v_\sigma} \right) (v_\sigma l - i\sigma\omega) \text{Log}(v_\sigma l - i\sigma\omega) \right. \\ &+ \left(\frac{1}{c + v_\sigma} - \frac{1}{c} \right) (cl + i\sigma\omega) \text{Log}(cl + i\sigma\omega) - \left(\frac{1}{c - v_\sigma} - \frac{1}{c} \right) (cl - i\sigma\omega) \text{Log}(cl - i\sigma\omega) \\ &\left. - 2 \frac{i\sigma\omega - v_\sigma l}{c + v_\sigma} \log((c + v_\sigma)\Lambda_B) + 2 \frac{i\sigma\omega}{c} \log(c\Lambda_B) - 2 \frac{i\sigma\omega - v_\sigma l}{c + v_\sigma} + 2 \frac{i\sigma\omega}{c} + \mathcal{O}(\omega/\Lambda_B, l/\Lambda_B) \right\}, \end{aligned} \quad (55)$$

with $\sigma = \pm$. When substituted into Eq. (48) in favor for $\bar{G}_\pm^{-1}(k)$, Eq. (55) leads to the UV logarithmic divergence in the linear coefficients of the frequency ω and the one-dimensional momentum l ;

$$\begin{aligned} \bar{G}_\pm^{-1}(k) &= \bar{G}_{\pm,0}^{-1}(k) + (\delta_\pm i\omega \mp \delta v_\pm l) \\ &+ (\dots) \ln \Lambda i\omega + (\dots) \ln \Lambda l + \dots \end{aligned}$$

Eq. (55) also has the weak IR singularity ($\omega \ln \omega$ type), that is controlled by the RG scale variable κ in Eq. (45) with ω or $v_\pm l = \kappa$.

Calculation of $\int_k \bar{G}_{+,0}(k+q) \bar{G}_{-,0}(k)$ and $\int_q \bar{G}_{\phi,0}(q)$ at $d = 3$

The 1-loop terms in the boson self-energy have two contributions (Fig. 4(b,c)). One with an integral over internal boson loop (Fig. 4(c)), and the other with an integral over internal fermion loop (Fig. 4(b)). The integral over the boson loop does not depend on external

momentum and frequency,

$$\begin{aligned} \int_q \bar{G}_{\phi,0}(q) &= \frac{1}{c^3} \int_{-\infty}^{+\infty} \frac{d\varepsilon}{2\pi} \int_{|\mathbf{q}| < \Lambda_B} \frac{d\mathbf{q}}{(2\pi)^3} \frac{1}{\varepsilon^2 + c^2 \mathbf{q}^2 + m^2} \\ &\rightarrow \frac{\Lambda_B^2}{16\pi^2 c^3} \quad (m \rightarrow 0). \end{aligned} \quad (56)$$

The integral over the fermion loop has the logarithmic divergence in the ultraviolet cutoff. To see this UV divergence, integrate first an angle between the internal fermion momentum and external boson momentum, θ ,

$$\begin{aligned} \int_k \bar{G}_{+,0}(k+q) \bar{G}_{-,0}(k) &= k_F^2 \int \frac{d^2 \hat{\Omega}}{(2\pi)^2} \\ &\int_{-\Lambda_F}^{+\Lambda_F} \frac{dl}{2\pi} \int_{-\Lambda_F}^{+\Lambda_F} \frac{d\omega}{2\pi} \frac{1}{i\omega - v_+ l} \frac{1}{i(\omega + \varepsilon) + v_- (l + m)} \\ &= \frac{1}{2\pi} \frac{k_F^2}{v_- q} \int_{-\Lambda_F}^{+\Lambda_F} \frac{dl}{2\pi} \int_{-\Lambda_F}^{+\Lambda_F} \frac{d\omega}{2\pi} \\ &\frac{1}{i\omega - v_+ l} \text{Log} \left[\frac{i(\omega + \varepsilon) + v_- l + v_- q}{i(\omega + \varepsilon) + v_- l - v_- q} \right], \end{aligned} \quad (57)$$

where $k \equiv (\omega, \mathbf{k})$, $\mathbf{k} \equiv (k_F + l)\hat{\Omega}$, $q \equiv (\varepsilon, \mathbf{q})$, and $\mathbf{q} \cdot \hat{\Omega} = q \cos \theta = m$ (Henceforth we will often write $|\mathbf{q}|$ as q , as far as the scalar $|\mathbf{q}|$ can be obviously distinguishable from the four-dimensional $q = (\varepsilon, \mathbf{q})$). For simplicity, we consider the case with $v_+ = v_- = v$, while putting only the result for the general case ($v_+ \neq v_-$) in Eq. (60). By choosing $v\Lambda_F = \bar{\Lambda}_F$, we introduce $Q/z \equiv \omega + ivl$ with $Q^2 \equiv \omega^2 + (vl)^2$;

$$\int_k \bar{G}_{+,0}(k+q) \bar{G}_{-,0}(k) \Big|_{v_+=v_-=v} = -\frac{1}{2\pi} \frac{k_F^2}{v^2 q} \times \int_0^{\bar{\Lambda}_F} \frac{dQ}{2\pi} \oint_{|z|=1} \frac{dz}{2\pi} \text{Log} \left[\frac{iz + (i\varepsilon + vq)/Q}{iz + (i\varepsilon - vq)/Q} \right]. \quad (58)$$

As a function of the complex variable z , the integrand in the right hand side has a branch cut from $z = -\xi \equiv -(\varepsilon + ivq)/Q$ to $z = -\xi^* \equiv -(\varepsilon - ivq)/Q$. For $Q < \varepsilon$, the z -integral along the unit circle is contractible. For

$\varepsilon < Q < R \equiv \sqrt{\varepsilon^2 + (vq)^2}$, the z -integral along the unit circle is contracted into an integral along a part of the branch cut. Thereby, the integral runs along one side and the other side of a line, that runs from $z = z_0 \equiv -\varepsilon/Q + i\sqrt{1 - (\varepsilon/Q)^2}$ to $z = z_0^*$ with $|z_0| = 1$. For $R < Q$, the z -integral along the unit circle can be contracted into an integral along a loop, that goes around the whole branch cut. That says, the integral reduces to

$$\begin{aligned} & \int_k \bar{G}_{+,0}(k+q) \bar{G}_{-,0}(k) \Big|_{v_+=v_-=v} \\ &= \frac{i}{4\pi^2} \frac{k_F^2}{v^2 q} \left(\int_R^{\bar{\Lambda}_F} dQ (-\xi^* + \xi) + \int_\varepsilon^R dQ (z_0 - z_0^*) \right) \\ &= -\frac{k_F^2}{2\pi^2 v} \left\{ \log \left(\frac{\bar{\Lambda}_F}{R} \right) + 1 - \frac{\varepsilon}{vq} \text{ArcTan} \left(\frac{vq}{\varepsilon} \right) \right\}. \quad (59) \end{aligned}$$

In the general case of $v_+ \neq v_-$, Eq. (57) can be similarly evaluated. The result is

$$\begin{aligned} & \int_k \bar{G}_{+,0}(k+q) \bar{G}_{-,0}(k) = \\ & -\frac{k_F^2}{\pi^2(v_+ + v_-)} \left\{ \log \left(\frac{\bar{\Lambda}_F}{R} \right) + 1 - \frac{\varepsilon}{v_- q} \frac{(v_+ + v_-)}{2v_+} \text{ArcTan} \left[\frac{v_- q}{\varepsilon} \right] - \frac{\varepsilon}{2v_+ q} \text{ArcTan} \left[\frac{(v_+ - v_-) \sin 2\theta}{(v_+ + v_-) - (v_+ - v_-) \cos 2\theta} \right] \right. \\ & \left. - \frac{1}{4} \log \left[\frac{(v_+ + v_-)^2 + (v_+ - v_-)^2 - 2(v_+ + v_-)(v_+ - v_-) \cos 2\theta}{(v_+ + v_-)^2} \right] \right\} + \mathcal{O}(q/\Lambda_F), \quad (60) \end{aligned}$$

with $\bar{\Lambda}_F \equiv v_- \Lambda_F$, $R^2 \equiv \varepsilon^2 + v_-^2 q^2$ and $(\cos \theta, \sin \theta) \equiv (\varepsilon, v_- q)/R$. In Eq. (49) in favor for $\bar{G}_\phi^{-1}(q)$, Eqs. (59,60) bring the UV logarithmic divergence into the boson mass. The UV divergence comes with the IR logarithmic divergence;

$$\begin{aligned} \bar{G}_\phi^{-1}(q) &= \bar{G}_{\phi,0}^{-1}(q) + (\delta m^2 + \delta c^2 q^2 + \delta_\phi \varepsilon^2) \\ &+ (\dots) k_F^2 \log \left(\frac{\Lambda}{R} \right) + \dots, \end{aligned}$$

with $R^2 \equiv \varepsilon^2 + (vq)^2$. The IR divergence is controlled by the RG scale variable κ in Eq. (45), where R is replaced by κ .

Calculation of the boson and fermion integrals in Eq. (51) at $d = 3$

The 1-loop term in the four-point boson vertex function has two contributions (Fig. 4(d,e)). The 1-loop term with the internal fermion integral has the IR quadratic divergence (Fig. 4(e)). To see this, set only the external boson frequencies to be finite, $q_i = (p_i, \mathbf{0})$, and integrate

over the fermion frequency ω ,

$$\begin{aligned} & \int_k \bar{G}_{+,0}(k) \bar{G}_{-,0}(k+q_1) \\ & \times \bar{G}_{+,0}(k+q_1-q_3) \bar{G}_{-,0}(k+q_1+q_2-q_3) \\ &= -i \frac{k_F^2}{\pi(v_+ + v_-)} \int_{-\infty}^{+\infty} \frac{dX}{2\pi} \left\{ \frac{1}{X + ip_1} \frac{1}{X + ip_3} \frac{1}{p_2 - p_3} \right. \\ & \left. + \frac{1}{X + ip_2} \frac{1}{X + ip_4} \frac{1}{-p_2 + p_3} \right\} \quad (61) \end{aligned}$$

with $k \equiv (\omega, \mathbf{k})$, $\mathbf{k} \equiv (k_F + l)\hat{\Omega}$ and $X \equiv (v_+ + v_-)l$. Here $p_1, p_2, p_3, p_4 = p_1 + p_2 - p_3$ are external boson frequencies of q_1, q_2, q_3 and q_4 respectively. When these frequencies are chosen with either $\text{sgn}(p_1 p_3) < 0$ or $\text{sgn}(p_2 p_4) < 0$, the integral over the one-dimensional fermion momentum $l \equiv X/(v_+ + v_-)$ gives a quadratic divergent term in the small external frequencies. When these frequencies are chosen with $\text{sgn}(p_1 p_3) > 0$ and $\text{sgn}(p_2 p_4) > 0$ as in Eq. (46), the integral over X leads to zero.

The 1-loop term with the internal boson integral has the UV logarithmic divergence (Fig. 4(d)). In the massless case ($m = 0$), the UV divergence comes with an IR logarithmic divergence. The IR divergence can be con-

trolled by choosing the external boson frequencies as in Eqs. (46,47). Thereby, the external boson frequencies play role of the RG scale variable κ ,

$$\begin{aligned} & \int_q \bar{G}_{\phi,0}(q) \bar{G}_{\phi,0}(q_1 + q_2 - q) \\ &= \int_{-\infty}^{+\infty} \frac{d\varepsilon}{2\pi} \int_{|q| < \Lambda_B} \frac{d^3 \mathbf{q}}{(2\pi)^3} \frac{1}{\varepsilon^2 + c^2 \mathbf{q}^2} \frac{1}{(\varepsilon - y)^2 + c^2 \mathbf{q}^2} \\ &= \frac{\log\left(\frac{2c\Lambda_B}{y}\right)}{8\pi^2 c^3} + \mathcal{O}(\Lambda_B^{-2}). \end{aligned} \quad (62)$$

Here $y = 4\kappa/3$ for the first term in Eq. (51) (particle-particle channel) and $y = \kappa/3$ for the other two in Eq. (51) (particle-hole channel). When substituted into Eq. (51) in favor for $\bar{\Gamma}_\lambda$, Eq. (62) leads to the UV logarithmic divergence in the ϕ^4 coupling,

$$\begin{aligned} & \bar{\Gamma}_\lambda(q_1, q_2, q_3) \Big|_{q_1=(\kappa,0), q_2=(\kappa/3,0), q_3=(2\kappa/3,0)} \\ &= -\lambda - \delta\lambda + (\dots) \log\left(\frac{\Lambda}{\kappa}\right) + \dots \end{aligned}$$

determination of the counterterms and β functions

By substituting Eqs. (55,56,60,62) into Eqs. (48,49,51) and imposing the conditions Eq. (45) on the renormalized vertex functions, we determine the counterterms in S_c ; δm^2 , δc^2 , δ_ϕ , δ_\pm , δv_\pm , δg and $\delta\lambda$. The counterterms are given as functions of the renormalized physical quantities, m^2 , c^2 , v_\pm , g , λ , the RG scale κ , the Fermi wavelength k_F and the UV cutoff Λ . So are the bare quantities, m_0^2 , c_0^2 , $v_{\pm 0}$, g_0 , λ_0 , and the renormalization of the field operator

amplitudes, Z_ϕ and Z_\pm ;

$$\begin{cases} m_0^2 = M_0^2(m^2, c^2, v_+, v_-, g, \lambda, \kappa, k_F, \Lambda), \\ c_0^2 = C_0^2(m^2, c^2, \dots, g, \lambda, \kappa, k_F, \Lambda), \\ v_{\sigma 0} = V_{\sigma 0}(m^2, c^2, \dots, g, \lambda, \kappa, k_F, \Lambda), \\ g_0 = G_0(m^2, c^2, \dots, g, \lambda, \kappa, k_F, \Lambda), \\ \lambda_0 = \Lambda_0(m^2, c^2, \dots, g, \lambda, \kappa, k_F, \Lambda), \end{cases} \quad (63)$$

and

$$\begin{cases} Z_\phi = Z_\phi(m^2, c^2, v_+, v_-, g, \lambda, \kappa, k_F, \Lambda), \\ Z_\sigma = Z_\sigma(m^2, c^2, \dots, g, \lambda, \kappa, k_F, \Lambda), \end{cases} \quad (64)$$

with $\sigma = \pm$. Eqs. (63,64) define a relation between bare quantities and renormalized physical quantities, in which all the universal information of the quantum criticality are encoded. To decode the information of the criticality, Eq. (43) and their derivative with respect to the RG scale variable κ are used in combination with Eqs. (63,64) (see Sec. IIG, IIH, Sec. III).

The renormalized perturbation theory determines Eqs. (63,64) perturbatively in g^2 and λ . In the paper, we shall focus only on the relation at the massless point, and set the renormalized physical mass m to be zero in Eqs. (63,64). Thereby, the first line of Eq. (63) defines a subspace of the quantum critical ‘point’ in a multiple-dimensional parameter space subtended by the bare quantities, m_0 , c_0 , $v_{\sigma 0}$, g_0 , λ_0 , and the RG scale variable κ ;

$$m_0^2 = M_0^2(m^2 = 0, c^2, v_+, v_-, g, \lambda, \kappa, k_F, \Lambda). \quad (65)$$

Meanwhile, the other relations in Eqs. (63,64) with $m^2 = 0$ define the critical properties at the quantum critical point;

$$\begin{cases} c_0^2 = C_0^2(m^2 = 0, c^2, v_+, v_-, g, \lambda, \kappa, k_F, \Lambda), \\ v_{\sigma 0} = V_{\sigma 0}(m^2 = 0, c^2, \dots, \lambda, \kappa, k_F, \Lambda), \\ g_0 = G_0(m^2 = 0, c^2, \dots, \lambda, \kappa, k_F, \Lambda), \\ \lambda_0 = \Lambda_0(m^2 = 0, c^2, \dots, \lambda, \kappa, k_F, \Lambda), \\ Z_\phi = Z_\phi(m^2 = 0, c^2, \dots, \lambda, \kappa, k_F, \Lambda), \\ Z_\sigma = Z_\sigma(m^2 = 0, c^2, \dots, \lambda, \kappa, k_F, \Lambda). \end{cases} \quad (66)$$

To be more specific, at the critical point ($m = 0$), the counterterms in S_c are given as functions of renormalized physical quantities, κ , k_F , and Λ perturbatively in g^2 and λ ;

$$\delta m^2 + \delta_\phi \kappa^2 - \frac{g^2 k_F^2}{\pi^2 (v_+ + v_-)} \left\{ \log\left(\frac{\bar{\Lambda}_F}{\kappa}\right) - \frac{1}{2} \log\left(\frac{2v_-}{v_+ + v_-}\right) \right\} + \frac{\lambda \Lambda_B^2}{16\pi^2 c^3} = 0, \quad (67)$$

$$\begin{cases} \delta_\sigma = -\frac{g^2}{8\pi^2 c v_\sigma} \left\{ \frac{2v_\sigma}{(c+v_\sigma)c} \log\left(\frac{\Lambda_B}{\kappa}\right) - \frac{2}{c+v_\sigma} \log(c+v_\sigma) + \frac{2}{c} \log c \right\} \\ \delta v_\sigma = -\frac{g^2}{8\pi^2 c v_\sigma} \left\{ \frac{2v_\sigma}{c+v_\sigma} \log\left(\frac{v_\sigma \Lambda_B}{\kappa}\right) + \frac{2v_\sigma}{c+v_\sigma} \log(c+v_\sigma) - \frac{2v_\sigma}{c+v_\sigma} \frac{1}{c-v_\sigma} (c \log c - v_\sigma \log v_\sigma) \right\}, \\ \delta\lambda = \frac{\lambda^2}{16\pi^2 c^3} \left\{ 5 \log\left(\frac{3c\Lambda_B}{\kappa}\right) + 3 \log 2 \right\}, \quad \delta_\phi = 0, \quad \delta c^2 = 0, \quad \delta g = 0. \end{cases} \quad (68)$$

with $\bar{\sigma} = \mp$ for $\sigma = \pm$. Here the followings were used from Eq. (60),

$$\frac{\partial}{\partial \varepsilon} \left(\int_k \bar{G}_{+,0}(k+q) \bar{G}_{-,0}(k) \right) \Big|_{\varepsilon=\kappa, q=0} = \frac{\partial}{\partial(c|\mathbf{q}|)} \left(\int_k \bar{G}_{+,0}(k+q) \bar{G}_{-,0}(k) \right) \Big|_{\varepsilon=0, c|\mathbf{q}|=\kappa} = \frac{k_F^2}{\pi^2(v_+ + v_-)\kappa}. \quad (69)$$

When substituted in Eqs. (49,45), Eq. (69) cancels the first order term in k_F^2 in the right hand side of the conditions for the boson self energy in Eq. (45).

In terms of Eqs. (68,67) and $m = 0$, a set of the bare physical quantities, $m_0, c_0, v_{\sigma 0}, g_0, \lambda_0$, are given as functions of renormalized physical quantities, the RG scale variable κ , the Fermi wavelength k_F and the UV cutoff Λ ,

$$m_0^2 = Z_\phi^{-1}(m^2 + \delta m^2) = \delta m^2 = -\frac{\lambda \Lambda_B^2}{16\pi^2 c^3} + \frac{g^2 k_F^2}{\pi^2(v_+ + v_-)} \left\{ \log\left(\frac{\bar{\Lambda}_F}{\kappa}\right) - \frac{1}{2} \log\left(\frac{2v_-}{v_+ + v_-}\right) \right\} + \dots \quad (70)$$

$$v_{\sigma 0} = Z_\sigma^{-1}(v_\sigma + \delta v_\sigma) = v_\sigma - \delta_\sigma v_\sigma + \delta v_\sigma + \dots, \quad (71)$$

$$c_0^2 = c^2 + \dots, \quad \lambda_0 = \lambda + \delta\lambda, \quad (72)$$

$$g_0 = (1 - \frac{1}{2}\delta_\phi)(1 - \frac{1}{2}\delta_+)(1 - \frac{1}{2}\delta_-)g \\ = (1 - \frac{1}{2}\delta_+ - \frac{1}{2}\delta_-)g + \dots, \quad (73)$$

with $\sigma = \pm$. Here $\delta_\sigma, \delta v_\sigma, \delta\lambda$ in the right hand sides are given in Eq. (68). ‘ \dots ’ in the right hand sides stands for the higher-order contributions in g^2 and λ . By inverse solutions of Eqs. (71,72,73,68), c, v_\pm, g, λ are given as functions of $c_0, v_{\pm 0}, g_0, \lambda_0, \kappa, k_F$ and Λ . On substitution of such solutions into Eq. (70), m_0 is given as a function of $c_0, v_{\pm 0}, g_0, \lambda_0, \kappa, k_F$ and Λ . Such a function for m_0 defines a subspace of $m = 0$ in a multiple-dimensional parameter space subtended by the bare physical quantities and the RG scale variable κ . The subspace of $m = 0$ defines the quantum critical ‘point’ in the parameter space of the bare quantities and κ .

Let us introduce a derivative with respect to the RG scale κ within the subspace of $m = 0$ and with fixed values of the other bare quantities, k_F and the UV cutoff;

$$\frac{\partial}{\partial \ln \kappa} \Big|_{c_0, v_{\pm 0}, g_0, \lambda_0, k_F, \Lambda: \text{fixed}} \equiv \frac{\partial}{\partial \ln \kappa} \Big|_{\dots}. \quad (74)$$

The following identities hold true trivially;

$$\frac{\partial c_0}{\partial \ln \kappa} \Big|_{\dots} = \frac{\partial v_{\sigma 0}}{\partial \ln \kappa} \Big|_{\dots} = \frac{\partial g_0}{\partial \ln \kappa} \Big|_{\dots} = \frac{\partial \lambda_0}{\partial \ln \kappa} \Big|_{\dots} = 0, \quad (75)$$

with $\sigma = \pm$. On application of such $\ln \kappa$ -derivative onto Eqs. (71,72,73) with Eq. (75) in their left hand sides, β functions of the physical quantities are obtained as their $\ln \kappa$ -derivatives. The β functions are calculated perturbatively in the Yukawa coupling g^2 and the ϕ^4 coupling

λ ,

$$\frac{\partial v_\sigma}{\partial \ln \kappa} \Big|_{\dots} = \frac{\partial \delta_\sigma}{\partial \ln \kappa} v_\sigma - \frac{\partial \delta v_\sigma}{\partial \ln \kappa} + \mathcal{O}(g^4, g^2 \lambda, \lambda^2) \\ = \frac{g^2}{4\pi^2 c(c + v_{\bar{\sigma}})} \left(\frac{v_\sigma}{c} - 1 \right) + \dots \equiv \beta_{v_\sigma}(c, \dots), \quad (76)$$

$$\frac{\partial c}{\partial \ln \kappa} \Big|_{\dots} = 0 + \dots \equiv \beta_c(c, \dots), \quad (77)$$

$$\frac{\partial g}{\partial \ln \kappa} \Big|_{\dots} = \frac{g}{2} \left(\frac{\partial \delta_+}{\partial \ln \kappa} + \frac{\partial \delta_-}{\partial \ln \kappa} \right) + \mathcal{O}(g^5, g^3 \lambda, g \lambda^2) \\ = \frac{g^3}{8\pi^2 c^2} \left(\frac{1}{c + v_+} + \frac{1}{c + v_-} \right) + \dots \equiv \beta_g(c, \dots), \quad (78)$$

$$\frac{\partial \lambda}{\partial \ln \kappa} \Big|_{\dots} = \frac{5\lambda^2}{16\pi^2 c^3} + \mathcal{O}(\lambda^3, \lambda^2 g^2, \lambda g^4, g^6) \equiv \beta_\lambda(c, \dots), \quad (79)$$

with $\sigma = \pm$ and $\bar{\sigma} = \mp$. Here ‘ \dots ’ in the right hand side refers to the higher-order terms in g^2 and λ . Importantly, the β functions are given only by the renormalized physical quantities themselves.

The leading-order β functions of g as well as λ dictate that in the low-energy limit ($\ln \kappa \rightarrow -\infty$), the Yukawa coupling g and ϕ^4 coupling λ are renormalized into the zero. The marginal irrelevance of g and λ in the IR limit justifies a posteriori the perturbative calculation in small g^2 and λ . The β functions of the two Fermi velocities shows that in the IR limit, both v_+ and v_- are renormalized into the same critical velocity as the boson velocity c . Within the one-loop level, the boson velocity has no renormalization; $\beta_c = 0$.

derivation of Callan-Symanzik equation for the two-point fermion Green's functions

The β functions appear in the Callan-Symanzik (CS) equations for the renormalized Green's functions. The role of the β functions become more significant, when the CS equations are solved in favor for the Green's functions [53, 54]. In this section, the CS equation for the fermion Green's functions will be derived. In the next section, the CS equations are solved in favor for the renormalized fermion Green's functions.

Let us begin with the relation between the renormalized fermion Green's function and the bare one. From

Eq. (43), the relation is,

$$\begin{aligned} Z_\sigma(m^2 = 0, c^2, v_+, v_-, g, \lambda, \kappa, \Lambda) \\ \times \bar{G}_\sigma(k; m^2 = 0, c^2, v_+, v_-, g, \lambda, \kappa) \\ = G_\sigma(k; m_0^2, c_0^2, v_{+0}, v_{-0}, g_0, \lambda_0, \Lambda). \end{aligned} \quad (80)$$

Here the k_F -dependence was trivially omitted, and will be omitted henceforth unless dictated otherwise. In Eq. (80), Z_σ and \bar{G}_σ in the left hand sides are given as functions of the renormalized physical quantities, c , v_\pm , g , λ , the RG scale variable κ and the UV cutoff Λ . By Eqs. (71,72,73,68), such renormalized physical quantities are given as functions of c_0 , $v_{\pm 0}$, g_0 , λ_0 , the RG scale variable κ , and Λ . G_σ in the right hand side is originally given as a function of m_0 , c_0 , $v_{\pm 0}$, g_0 , λ_0 and the UV cutoff Λ . By Eq. (70) with Eqs. (71,72,73,68), m_0 is given by c_0 , $v_{\pm 0}$, g_0 , λ_0 , the RG scale variable κ , and Λ . With this in mind, take the κ -derivative of Eq. (80) with respect to Eq. (74). The derivative gives the following inhomogeneous CS equation

$$\begin{aligned} \left\{ \frac{\partial}{\partial \ln \kappa} + \beta_c \frac{\partial}{\partial c} + \sum_{\sigma'=\pm} \beta_{v_{\sigma'}} \frac{\partial}{\partial v_{\sigma'}} + \beta_g \frac{\partial}{\partial g} + \beta_\lambda \frac{\partial}{\partial \lambda} \right. \\ \left. + \gamma_\sigma \right\} \bar{G}_\sigma(k; m^2 = 0, c^2, \dots, \lambda, \kappa) = \frac{\partial m_0^2}{\partial \ln \kappa} \frac{\partial G_\sigma}{\partial m_0^2}. \end{aligned} \quad (81)$$

Here γ_σ ($\sigma = \pm$) is called as γ function and it is given by the κ -derivative of the renormalizations of the field operator amplitudes,

$$\begin{aligned} \left. \frac{\partial \ln Z_\sigma}{\partial \ln \kappa} \right|_{\dots} &= \left. \frac{\partial \ln(1 + \delta_\sigma)}{\partial \ln \kappa} \right|_{\dots} \\ &= \frac{g^2}{4\pi^2 c^2 (c + v_{\bar{\sigma}})} + \mathcal{O}(g^4, g^2 \lambda, \lambda^2) \equiv \gamma_\sigma. \end{aligned} \quad (82)$$

with $\sigma = \pm$ and $\bar{\sigma} = \mp$.

Note that the right hand side of Eq. (81) is at most on the order of $\mathcal{O}(g^4)$ and negligible within the one-loop level calculation. Namely, Eq. (70) leads to

$$\left. \frac{\partial m_0^2}{\partial \ln \kappa} \right|_{\dots} = -\frac{g^2 k_F^2}{\pi^2 (v_+ + v_-)} + \mathcal{O}(g^4, g^2 \lambda, \lambda^2). \quad (83)$$

The partial derivative of the bare fermion Green's function with respect to the bare boson mass results in an amputated 1PI connected Green's function with two boson lines and two fermion lines. Such is at most on the order of $\mathcal{O}(g^2)$ too;

$$\begin{aligned} \frac{\partial G_\sigma(k)}{\partial m_0^2} &= G_\sigma(k) \frac{\partial G_\sigma^{-1}(k)}{\partial m_0^2} G_\sigma(k) \\ &\equiv \int_q G_\sigma(k) \Gamma_\sigma^{(2,2)}(k, k; q, q) G_\sigma(k) = \mathcal{O}(g^2). \end{aligned} \quad (84)$$

Here $\Gamma_\sigma^{(2,2)}(k, k; q, q)$ is the amputated 1PI connected Green's function with two external bosons and two external fermions lines (Fig. 4(f)). From Eqs. (83,84), the

right hand side of Eq. (81) can be neglected within the one-loop order;

$$\begin{aligned} \left\{ \frac{\partial}{\partial \ln \kappa} + \sum_{\sigma'=\pm} \beta_{v_{\sigma'}} \frac{\partial}{\partial v_{\sigma'}} + \beta_g \frac{\partial}{\partial g} \right. \\ \left. + \gamma_\sigma \right\} \bar{G}_\sigma(l, \omega; m^2 = 0, c^2, \dots, \kappa) = \mathcal{O}(g^4, g^2 \lambda, \lambda^2), \end{aligned} \quad (85)$$

with $k \equiv (\mathbf{k}, \omega)$ and $\mathbf{k} \equiv (k_F + l)\Omega$. Here those terms with ∂_c and ∂_λ are omitted from the left hand side in Eq. (81), because $\beta_c = 0$ and \bar{G}_σ does not depend on λ within the one-loop order. In the next section, we shall solve this homogeneous CS equation in favor for the renormalized fermion Green's functions.

derivation of Callan-Symanzik equation for the two-point boson Green's function

In this section, the CS equation for the two-point boson Green's function will be derived. As in the previous section, let us begin with the relation between the bare and renormalized function;

$$\begin{aligned} Z_\phi^{-1}(m^2 = 0, c^2, \dots, \lambda, \kappa, \Lambda) \bar{G}_\phi^{-1}(q; c^2, \dots, \lambda, \kappa) \\ = G_\phi^{-1}(q; m_0^2, c_0^2, \dots, \lambda_0, \Lambda). \end{aligned} \quad (86)$$

The κ -derivative of Eq. (74) leads to the following inhomogeneous equation,

$$\begin{aligned} \left\{ \frac{\partial}{\partial \ln \kappa} + \beta_c \frac{\partial}{\partial c} + \sum_{\sigma=\pm} \beta_{v_\sigma} \frac{\partial}{\partial v_\sigma} + \beta_g \frac{\partial}{\partial g} + \beta_\lambda \frac{\partial}{\partial \lambda} \right. \\ \left. - \gamma_\phi \right\} \bar{G}_\phi^{-1}(q; m^2 = 0, c^2, \dots, \lambda, \kappa) = \frac{\partial m_0^2}{\partial \ln \kappa} \frac{\partial G_\phi^{-1}}{\partial m_0^2}. \end{aligned} \quad (87)$$

Note that in the leading order in g^2 and λ , the γ function for the boson Green's function is zero; $\gamma_\phi = \mathcal{O}(g^4, g^2 \lambda, \lambda^2)$. Meanwhile, the right hand side of Eq. (87) has a finite leading-order contribution, because $\partial G_\phi^{-1} / \partial m_0^2 = 1 + \mathcal{O}(g^2, \lambda)$. Thus, the CS equation takes an inhomogeneous form,

$$\begin{aligned} \left\{ \frac{\partial}{\partial \ln \kappa} + \sum_{\sigma=\pm} \beta_{v_\sigma} \frac{\partial}{\partial v_\sigma} + \beta_g \frac{\partial}{\partial g} \right\} \bar{G}_\phi^{-1}(q, c^2, \dots, \kappa) \\ = -\frac{g^2 k_F^2}{\pi^2 (v_+ + v_-)} + \mathcal{O}(g^4, g^2 \lambda, \lambda^2). \end{aligned} \quad (88)$$

Here we also omitted ∂_λ in the left hand side, which leads to terms on the order of $\mathcal{O}(\lambda^2)$; $\beta_\lambda \propto \mathcal{O}(\lambda^2)$. In the next section, this equation will be solved in favor for the two-point boson Green's function.

APPROXIMATE SOLUTIONS OF CALLAN-SYMANZIK EQUATIONS

The β functions for the fermion velocities suggest that the two fermion velocities are renormalized into the boson

velocities c in the infrared (IR) limit ($\ln \kappa \rightarrow -\infty$);

$$\frac{dv_{\pm}}{d \ln \kappa} = \frac{g^2}{4\pi^2 c(c + v_{\mp})} \left(\frac{v_{\pm}}{c} - 1 \right).$$

That says, at the quantum critical point ($m = 0$), the two fermion bands proximate to the Fermi surface have asymptotically the same critical velocity as the boson velocity. We thus assume that $v_{\pm} = c$ in the following analysis.

two-point fermion Green's function and spectral function

With $v_{\pm} = c$, the homogeneous CS equation for the fermion Green's function is given by

$$\left\{ \frac{\partial}{\partial \ln \kappa} + \beta_g(g) \frac{\partial}{\partial g} + \gamma_{\sigma}(g) \right\} \bar{G}_{\sigma}(l, \omega; g, \kappa) = 0. \quad (89)$$

The c and v_{\pm} -dependences of \bar{G}_{σ} , β_g and γ_{σ} can be trivially omitted; $\beta_{v_{\pm}} = \beta_c = 0$ at $v_{\pm} = c$. From a dimensional analysis, the fermion Green's function has the following scaling form,

$$G_{\sigma}(l, \omega; g, \kappa) = \frac{1}{i\omega - \sigma cl} f_{\sigma}(l/\kappa, \omega/\kappa; g), \quad (90)$$

with $\sigma = \pm$. Thus, with $\omega = p \sin \theta$ and $cl = p \cos \theta$, the κ -derivative is replaced by the p -derivative with fixed θ ;

$$\left\{ p \frac{\partial}{\partial p} - \beta_g(g) \frac{\partial}{\partial g} + (1 - \gamma_{\sigma}(g)) \right\} \bar{G}_{\sigma}(p, \theta; g, \kappa) = 0. \quad (91)$$

From Eqs. (78,82), β_g and γ_{σ} are given at $v_{\pm} = c$ as;

$$\beta_g(g) = \frac{g^3}{8\pi^2 c^3}, \quad \gamma_{\sigma}(g) = \frac{g^2}{8\pi^2 c^3}. \quad (92)$$

The solution of Eq. (91) is given by

$$\begin{aligned} \bar{G}_{\sigma}(p, \theta; g, \kappa) &= \bar{\mathcal{G}}_{\sigma}(\theta; \bar{g}(t; g), \kappa) \\ &\times \exp \left[\int_{\bar{g}(t; g)}^g \frac{1 - \gamma_{\sigma}(g')}{\beta_g(g')} dg' \right], \end{aligned} \quad (93)$$

with $t \equiv \ln(p/\kappa)$. $\bar{\mathcal{G}}_{\sigma}(\theta; g, \kappa)$ is the Green's function at $p = \kappa$ ($t = 0$);

$$\bar{G}_{\sigma}(p = \kappa, \theta; g, \kappa) \equiv \bar{\mathcal{G}}_{\sigma}(\theta; g, \kappa). \quad (94)$$

$\bar{g}(t; g)$ is a running coupling constant determined by a one-parameter scaling equation with β_g ;

$$\frac{\partial \bar{g}(t; g)}{\partial t} = \beta_g(\bar{g}) = \frac{\bar{g}^3}{8\pi^2 c^3}, \quad \bar{g}(t = 0; g) = g. \quad (95)$$

The running coupling constant becomes renormalized into the smaller value in the IR limit,

$$\bar{g}(t; g) = g \sqrt{\frac{1}{1 - g^2 \frac{t}{4\pi^2 c^3}}}. \quad (96)$$

Namely, for $p \ll \kappa$, $t = \ln(p/\kappa)$ is negative and logarithmically large. \bar{g}/g goes to the zero in the low-energy limit ($p \ll \kappa$). Thus, for smaller p in Eq. (93), $\bar{\mathcal{G}}_{\sigma}(\theta; \bar{g}, \kappa)$ in its right hand side might be evaluated perturbatively in the small \bar{g} . Eq. (48) with $v_{\pm} = c$ gives the second order expression for $\bar{G}_{\sigma}(l, \omega; g, \kappa)$ for small g ,

$$\begin{aligned} \bar{G}_{\sigma}^{-1}(l, \omega; g, \kappa) &= (i\omega - \sigma cl) \\ &- \frac{g^2}{8\pi^2 c^3} (i\omega - \sigma cl) \left\{ \log \left[\frac{\sqrt{(cl)^2 + \omega^2}}{\kappa} \right] - 1 \right\}, \end{aligned} \quad (97)$$

at $v_{\pm} = c$. Here the following relations are used from Eqs. (55,68),

$$\begin{aligned} \lim_{v_{\pm} \rightarrow c} \int_q \bar{G}_{\sigma}(k+q) \bar{G}_{\phi}(q) \Big|_{m=0} \\ = -\frac{\sigma}{8\pi^2 c^2} \left\{ -\frac{1}{2c} (cl + i\sigma\omega) \log (cl + i\sigma\omega) \right. \\ \left. - \frac{1}{2c} (cl + i\sigma\omega) \log (cl - i\sigma\omega) + \frac{i\sigma\omega}{c} \right. \\ \left. - \frac{i\sigma\omega - cl}{c} \log 2 + \frac{i\sigma\omega + cl}{c} \log (c\Lambda_B) \right\}, \\ \lim_{v_{\pm} \rightarrow c} \delta_{\sigma} = -\frac{g^2}{8\pi^2 c^2} \left\{ \frac{1}{c} \log \left(\frac{\Lambda_B}{\kappa} \right) + \frac{1}{c} \log \left(\frac{c}{2} \right) \right\}, \\ \lim_{v_{\pm} \rightarrow c} \delta v_{\sigma} = -\frac{g^2}{8\pi^2 c^2} \left\{ \log \left(\frac{c\Lambda_B}{\kappa} \right) + \log 2 - 1 \right\}. \end{aligned} \quad (98)$$

A comparison between Eqs. (94,97) gives

$$\bar{\mathcal{G}}_{\sigma}^{-1}(\theta; \bar{g}, \kappa) = -\sigma \kappa e^{-\sigma i\theta} \left(1 + \frac{\bar{g}^2}{8\pi^2 c^3} \right). \quad (99)$$

Meanwhile, the exponential factor in Eq. (93) is calculated as

$$\begin{aligned} \exp \left[\int_{\bar{g}(t; g)}^g \frac{1 - \gamma_{\sigma}(g')}{\beta_g(g')} dg' \right] \\ = \exp \left[\int_t^0 dt' \right] \exp \left[- \int_{\bar{g}}^g \frac{1}{g'} dg' \right] = \frac{\kappa \bar{g}}{p g}. \end{aligned} \quad (100)$$

Thus, the renormalized fermion Green's function near the Fermi surface is obtained as

$$\bar{G}_{\sigma}(l, \omega; g, \kappa) = \frac{1}{i\omega - \sigma cl} \left(1 + \frac{\bar{g}^2}{8\pi^2 c^3} \right)^{-1} \sqrt{\frac{1}{1 - g^2 \frac{t}{4\pi^2 c^3}}}, \quad (101)$$

with $t \equiv \ln(\sqrt{(cl)^2 + \omega^2}/\kappa)$. \bar{g} in the right hand side is given by t and g by Eq. (96).

By an analytic continuation $i\omega \rightarrow \omega + i\delta$, the imaginary part of the retarded Green's function (fermion spectral function) is obtained;

$$\begin{aligned} \bar{G}_\sigma^R(l, \omega) &\equiv \bar{G}_\sigma(l, \omega)|_{i\omega \rightarrow \omega + i\delta} \\ \text{Im} \bar{G}_\sigma^R(l, \omega) &= \frac{\mathcal{P}}{\omega - \sigma cl} (\bar{A} \bar{D} - \bar{B} \bar{C}) \\ &\quad - \pi \delta(\omega - \sigma cl) (\bar{A} \bar{C} + \bar{B} \bar{D}), \end{aligned} \quad (102)$$

where

$$\begin{cases} \bar{A} \equiv \frac{(1-2\alpha A)^2 + \alpha(1-2\alpha A) + (2\alpha B)^2}{(1+\alpha-2\alpha A)^2 + (2\alpha B)^2}, \\ \bar{B} \equiv \frac{2\alpha^2 B}{(1+\alpha-2\alpha A)^2 + (2\alpha B)^2}, \\ \bar{C} \equiv \frac{\text{Cos}[\frac{1}{2} \text{Arg}(1-2\alpha A - i2\alpha B)]}{[(1-2\alpha A)^2 + (2\alpha B)^2]^{\frac{1}{4}}}, \\ \bar{D} \equiv -\frac{\text{Sin}[\frac{1}{2} \text{Arg}(1-2\alpha A - i2\alpha B)]}{[(1-2\alpha A)^2 + (2\alpha B)^2]^{\frac{1}{4}}}, \\ \alpha \equiv \frac{g^2}{8\pi^2 c^3}, \quad A \equiv \log \left[\frac{\sqrt{|(cl)^2 - \omega^2|}}{\kappa} \right], \\ B \equiv \frac{\pi}{2} [\theta(-\omega - |cl|) - \theta(\omega - |cl|)]. \end{cases} \quad (103)$$

Note that for low-energy fermions, $|(cl)^2 - \omega^2| \ll \kappa^2$ and A is negative definite. Thus, \bar{A} and \bar{C} are positive definite. B , \bar{B} and \bar{D} is positive (negative) definite for $\omega < 0$ ($\omega > 0$). Especially, when $\omega \rightarrow \pm cl \pm \eta$ with positive $\eta \ll \kappa$, A becomes negatively large and show a logarithmic divergence,

$$\lim_{\omega \rightarrow |cl| \pm \eta} A = \frac{1}{2} \log \eta + \dots \quad (104)$$

Because of the logarithmic divergence, the quasi-particle weight in the spectral function is zero. Namely, in the limit of $\eta = 0$ with $\omega^2 = (cl)^2 \pm 2(cl)\eta$,

$$\begin{aligned} \lim_{\eta \rightarrow 0} \bar{A} &= 1, \quad \lim_{\eta \rightarrow 0} \bar{B} = \frac{B}{2|A|^2}, \\ \lim_{\eta \rightarrow 0} \bar{C} &= \frac{1}{\sqrt{2\alpha|A|}}, \quad \lim_{\eta \rightarrow 0} \bar{D} = \frac{1}{\sqrt{2\alpha|A|}} \frac{B}{2|A|}, \\ \lim_{\eta \rightarrow 0} (\bar{A} \bar{C} + \bar{B} \bar{D}) &= \frac{1}{\sqrt{2\alpha|A|^{\frac{1}{2}}}} + \dots \rightarrow 0, \end{aligned} \quad (105)$$

$$\lim_{\eta \rightarrow 0} (\bar{A} \bar{D} - \bar{B} \bar{C}) = \frac{B}{2\sqrt{2\alpha|A|^{\frac{3}{2}}}} + \dots \rightarrow 0. \quad (106)$$

The spectral function is comprised only of continuum spectrum, that appears in $\omega > |cl|$ (Fig. 5). From Eqs. (102,106), the continuum spectrum of $\text{Im} \bar{G}_\sigma^R$ show a weak divergence at $\omega = \sigma cl$;

$$-\text{Im} \bar{G}_\sigma^R(l, \omega) = \begin{cases} \sqrt{\frac{1}{\alpha}} \frac{\pi}{2} \frac{1}{\eta} \frac{1}{[|\log \eta|]^{\frac{3}{2}}} & (\omega = \sigma cl + \eta) \\ 0 & (-\sigma cl < \omega < \sigma cl) \\ \sqrt{\frac{1}{\alpha}} \frac{\pi}{4\sigma cl} \frac{1}{[|\log \eta|]^{\frac{3}{2}}} & (\omega = -\sigma cl - \eta) \end{cases} \quad (107)$$

for $\sigma cl > 0$ and

$$-\text{Im} \bar{G}_\sigma^R(l, \omega) = \begin{cases} \sqrt{\frac{1}{\alpha}} \frac{\pi}{(-4\sigma cl)} \frac{1}{[|\log \eta|]^{\frac{3}{2}}} & (\omega = -\sigma cl + \eta) \\ 0 & (\sigma cl < \omega < -\sigma cl) \\ \sqrt{\frac{1}{\alpha}} \frac{\pi}{2} \frac{1}{\eta} \frac{1}{[|\log \eta|]^{\frac{3}{2}}} & (\omega = \sigma cl - \eta) \end{cases} \quad (108)$$

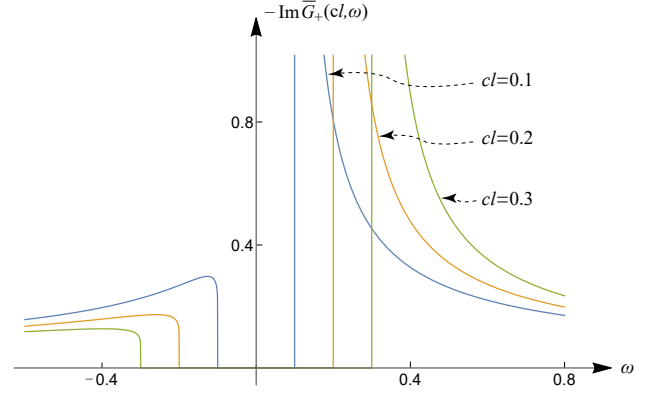


FIG. 5. Fermionic spectral function $-\text{Im} \bar{G}_+(l, \omega)$ as a function of the frequency ω for several l . Eq. (102) is plotted for $cl = 0.1$ (blue), $cl = 0.2$ (purple), $cl = 0.3$ (ocher). $\kappa = 1$, $\alpha = 0.1$, and the horizontal axis is ω .

for $\sigma cl < 0$ with $\sigma = \pm$. Note that the asymptotic behaviours of the fermion spectral function near the Fermi edge come from a factor of \bar{g}/g in Eq. (100); Eqs. (107,108) hold true even if $\bar{G}_\sigma^{-1}(\theta; \bar{g}, \kappa)$ in Eq. (99) is replaced by the free Green's function; $-\sigma \kappa e^{-i\sigma\theta}$.

When the temperature is finite, the quasi-particle spectral weight at $\omega = \sigma cl$ becomes finite in $\text{Im} \bar{G}^R$ and it is scaled by $\sqrt{\log T}$;

$$-\text{Im} \bar{G}_\sigma^R(l, \omega, T \neq 0) = \frac{\pi}{\sqrt{2\alpha}} \frac{1}{\sqrt{|\log T|}} \delta(\omega - \sigma cl) + \dots \quad (109)$$

To see this, one can go back to Eqs. (93,100,101) and note that the vanishing quasi-particle spectral weight at $T = 0$ comes from the vanishing \bar{g}/g in Eq. (100) in the limit of small $p^2 \equiv (cl)^2 - \omega^2 - 2i\omega\delta$. Such is true only at the zero temperature; at $T = 0$, one can countlessly renormalize at the quantum critical point, until small p is scaled up to the RG scale κ on the renormalization. At the finite temperature, however, the temperature as well as p is also scaled up to a larger value on the renormalization. Thus, the renormalization must be terminated, either when the renormalized temperature reaches a certain high temperature scale T_0 or when the renormalized p reaches the RG scale. This consideration naturally lets us replace \bar{g}/g in Eq. (100) by the following expression at $p = 0$ and at $T \neq 0$,

$$\begin{aligned} \left(\frac{\bar{g}}{g} \right) \Big|_{p=0, T \neq 0} &= \sqrt{\frac{1}{1 - 2\alpha t}} \Big|_{t=\log(\frac{T}{T_0})} \\ &\simeq \frac{1}{\sqrt{2\alpha}} \frac{1}{\sqrt{|\log T|}} + \dots \end{aligned} \quad (110)$$

Putting this back to Eq. (100,93) gives Eq. (109).

two-point boson Green's function and spectral function

With $v_{\pm} = c$, the CS equation for the two-point boson vertex function is given by

$$\left\{ \frac{\partial}{\partial \ln \kappa} + \beta_g(g) \frac{\partial}{\partial g} \right\} \bar{G}_{\phi}^{-1}(q; g, \kappa) = -\frac{g^2 k_F^2}{2\pi^2 c}. \quad (111)$$

Henceforth, we recover the implicit k_F -dependences in \bar{G}_{ϕ} . According to Eq. (35), we will expand \bar{G}_{ϕ}^{-1} in the powers of k_F^2 ;

$$\begin{aligned} \bar{G}_{\phi}^{-1}(q; g, \kappa) = & \bar{G}_{\phi,(0)}^{-1}(q; g, \kappa) + k_F^2 \bar{G}_{\phi,(1)}^{-1}(q; g, \kappa) \\ & + k_F^4 \bar{G}_{\phi,(2)}^{-1}(q; g, \kappa) + \dots \end{aligned} \quad (112)$$

The dimensional analysis dictates that $\bar{G}_{\phi,(n)}$ has a different scaling form for different n ;

$$\begin{aligned} \bar{G}_{\phi,(0)}^{-1}(q; g, \kappa) &= r^2 g_{(0)}^{-1}(r/\kappa, \theta; g), \\ \bar{G}_{\phi,(1)}^{-1}(q; g, \kappa) &= g_{(1)}^{-1}(r/\kappa, \theta; g), \\ \bar{G}_{\phi,(2)}^{-1}(q; g, \kappa) &= r^{-2} g_{(2)}^{-1}(r/\kappa, \theta; g), \dots \end{aligned} \quad (113)$$

with $q \equiv (\varepsilon, \mathbf{q})$, $c|\mathbf{q}| \equiv r \sin \theta$, $\varepsilon \equiv r \cos \theta$. Since β_g has no k_F dependence, the CS equation can be decomposed into equations at every order in k_F^2 ;

$$\begin{cases} \left\{ \frac{\partial}{\partial \ln \kappa} + \beta_g(g) \frac{\partial}{\partial g} \right\} (r^2 g_{(0)}^{-1}(r/\kappa, \theta; g)) = 0, \\ \left\{ \frac{\partial}{\partial \ln \kappa} + \beta_g(g) \frac{\partial}{\partial g} \right\} (g_{(1)}^{-1}(r/\kappa, \theta; g)) = -\frac{g^2}{2\pi^2 c}, \\ \left\{ \frac{\partial}{\partial \ln \kappa} + \beta_g(g) \frac{\partial}{\partial g} \right\} (r^{-2} g_{(2)}^{-1}(r/\kappa, \theta; g)) = 0, \\ \dots \end{cases} \quad (114)$$

In terms of Eq. (96), the CS equation at every order in k_F^2 can be solved in the leading order in g^2 . The solutions are

$$\begin{cases} g_{(0)}^{-1}(r/\kappa, \theta; g) = h_{(0)}(\theta; \bar{g}), \\ g_{(1)}^{-1}(r/\kappa, \theta; g) = -\frac{\bar{g}}{2\pi^2 c} (-t + h_1(\theta; \bar{g})), \\ g_{(2)}^{-1}(r/\kappa, \theta; g) = h_{(2)}(\theta; \bar{g}), \\ \dots \end{cases} \quad (115)$$

with $t \equiv \ln(r/\kappa)$. \bar{g} in the right hand side is given as a function of t and g by Eq. (96). This gives the two-point boson vertex function as follows,

$$\begin{aligned} \bar{G}_{\phi}^{-1}(r, \theta; g, \kappa) = & r^2 h_{(0)}(\theta; \bar{g}) \\ & - \frac{\bar{g} k_F^2}{2\pi^2 c} (-t + h_1(\theta; \bar{g})) + r^{-2} k_F^4 h_{(2)}(\theta; \bar{g}) + \dots \end{aligned} \quad (116)$$

According to Eqs. (116,96), $\bar{G}_{\phi}(r, \theta; g, \kappa)$ in the IR limit ($r \ll \kappa$) is determined by forms of $h_{(0)}(\theta; g)$, $h_{(1)}(\theta; g)$ and $h_{(2)}(\theta; g)$ for tiny g . To determine them for such small g , let us take $r = \kappa$ in Eq. (116) and expand its right

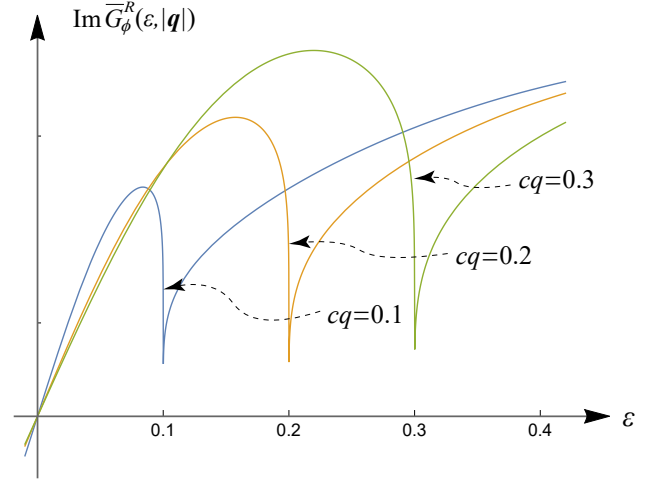


FIG. 6. Bosonic spectral function $\text{Im} \bar{G}_{\phi}^R(\varepsilon, |\mathbf{q}|)$ as a function of the frequency ε for several $|\mathbf{q}|$. Eq. (120) is plotted for $c|\mathbf{q}| = 0.1$ (blue), $c|\mathbf{q}| = 0.2$ (purple), $c|\mathbf{q}| = 0.3$ (ocher). $\kappa = 1$, $\alpha = 0.1$, $\gamma = 1$, and the horizontal axis is ε .

hand side in small $\bar{g}(t=0; g) = g$. For small g , $\bar{G}_{\phi}(r = \kappa, \theta; g, \kappa)$ in the left hand side may be calculated by the second order perturbation as;

$$\begin{aligned} \bar{G}_{\phi}^{-1}(r = \kappa, \theta; g, \kappa) = & \kappa^2 - \frac{g^2 k_F^2}{2\pi^2 c} \left(1 - \frac{\theta}{\tan \theta} \right) \\ & + \mathcal{O}(g^4, g^2 \lambda, \lambda^2). \end{aligned} \quad (117)$$

Here Eqs. (56,59,68) with $v_{\pm} = c$ are substituted into Eq.(49). A comparison between Eq. (117) and Eq. (116) at $r = \kappa$ determines $h_{(0)}(\theta; g)$, $h_{(1)}(\theta; g)$ and $h_{(2)}(\theta; g)$ for tiny g ;

$$\begin{aligned} h_{(0)}(\theta; g) &= 1, \quad h_{(1)}(\theta; g) = 1 - \frac{\theta}{\tan \theta}, \\ h_{(2)}(\theta; g) &= 0, \dots \end{aligned} \quad (118)$$

This leads to an expected result for the two-point boson vertex function in the IR limit ($r \ll \kappa$);

$$\bar{G}_{\phi}^{-1}(q; g, \kappa) = r^2 - \frac{\bar{g}^2 k_F^2}{2\pi^2 c} \left(-t + 1 - \frac{\theta}{\tan \theta} \right), \quad (119)$$

with $q = (\varepsilon, \mathbf{q})$, $\varepsilon = r \cos \theta$, $c|\mathbf{q}| = r \sin \theta$, $t \equiv \ln(r/\kappa)$. \bar{g} in the right hand side is given by t and g by Eq. (96). By comparing Eq. (119) with Eqs. (49,56,59,60), one can see that the Λ_B^2 term in the naive perturbation result is absorbed into the renormalization of the boson mass. $\text{Log } \bar{\Lambda}_F$ and the Yukawa coupling g in Eq. (49) are replaced by $\log \kappa$ and the IR-limit value of g , \bar{g} , respectively.

By an analytic continuation $i\varepsilon \rightarrow \varepsilon + i\delta$, the imaginary part of the retarded boson Green's function (boson

spectral function) is obtained as,

$$\begin{aligned} \overline{G}_\phi^R(\varepsilon, \mathbf{q}) &\equiv \overline{G}_\phi(\varepsilon, \mathbf{q}) \Big|_{i\varepsilon \rightarrow \varepsilon + i\delta}, \\ \text{Im}\overline{G}_\phi^R(\varepsilon, \mathbf{q}) &= \frac{\gamma \overline{F}}{(-\varepsilon^2 + c^2 \mathbf{q}^2 - \gamma \overline{E})^2 + \gamma^2 \overline{F}^2}, \end{aligned} \quad (120)$$

where \overline{E} , \overline{F} and γ are given as follows,

$$\begin{cases} \overline{E} = \frac{(1-2\alpha A)(1-A)+2\alpha B^2+2\alpha BB'}{(1-2\alpha A)^2+(2\alpha B)^2}, \\ \overline{F} = -\frac{(1-2\alpha A)B'+(1-2\alpha)B}{(1-2\alpha A)^2+(2\alpha B)^2}, \\ \alpha \equiv \frac{g^2}{8\pi^2 c^3}, \quad \gamma \equiv \frac{g^2 k_F^2}{2\pi^2 c}, \\ A \equiv \log \left[\frac{\sqrt{[(c|\mathbf{q}|)^2 - \varepsilon^2]}}{\kappa} \right], \\ B \equiv \frac{\pi}{2} [\theta(-\varepsilon - c|\mathbf{q}|) - \theta(\varepsilon - c|\mathbf{q}|)], \\ B' \equiv -\frac{\varepsilon}{c|\mathbf{q}|} \frac{\pi}{2} \theta(c|\mathbf{q}| - |\varepsilon|). \end{cases} \quad (121)$$

Note that the spectral weight is positive for $\varepsilon > 0$ and negative for $\varepsilon < 0$, for the low-energy boson, $|c^2 \mathbf{q}^2 - \varepsilon^2| \ll \kappa^2$, and for those Yukawa coupling smaller than a critical value ($\alpha < \frac{1}{2}$). Especially when $\varepsilon \rightarrow c|\mathbf{q}| + \eta$, ‘A’ becomes negatively large and diverges logarithmically. Due to this logarithmic divergence, the spectral weight has a ‘valley’ at $\varepsilon = c|\mathbf{q}|$ (Fig. 6), around which \overline{E} and \overline{F} take the following asymptotic forms,

$$\begin{aligned} \lim_{\varepsilon \rightarrow c|\mathbf{q}|} \overline{E} &= \frac{1}{2\alpha}, \quad \lim_{\varepsilon \rightarrow c|\mathbf{q}|} \overline{F} = \frac{B'}{2\alpha A} = \frac{\pi}{2} \frac{1}{\alpha |\log |\eta||}, \\ \lim_{\varepsilon \rightarrow c|\mathbf{q}|+} \overline{F} &= -\frac{(1-2\alpha)B}{4\alpha^2 A^2} = \frac{\pi}{2} \frac{1-2\alpha}{\alpha^2 |\log |\eta||^2}. \end{aligned} \quad (122)$$

The result shows that the delta-function peak at $\varepsilon = c|\mathbf{q}|$ for $g = 0$ is wiped out completely at small but finite g , and is replaced by the valley. The weight has broad peaks next to the valley. Toward the bottom of the valley, the spectral weight vanishes as

$$\text{Im}\overline{G}_\phi^R(\varepsilon, \mathbf{q}) = \begin{cases} \frac{2\pi}{\gamma} \frac{\alpha}{|\log \eta|} & (\varepsilon = c|\mathbf{q}| - \eta), \\ \frac{2\pi}{\gamma} \frac{1-2\alpha}{|\log \eta|^2} & (\varepsilon = c|\mathbf{q}| + \eta). \end{cases} \quad (123)$$

DENSITY OF STATES AND RESISTIVITY IN THE QUANTUM CRITICAL REGIME

The fermionic spectral function obtained in the previous section shows the breakdown of the ‘quasi-particle Fermi-liquid’ picture in the two-bands Fermi system coupled with the critical ϕ^4 boson [39, 40]. The result suggests the presence of a marginal-Fermi liquid (marginal-FL) regime in a high- T side of the quantum critical point (QCP). In this section, characteristic T -dependences of various physical quantities will be calculated in the marginal-FL regime. We first evaluate the density of states (DOS) near the Fermi level at the QCP. We next evaluate the fermion’s spectral function in the high- T side of the QCP (quantum critical regime; QCR). By using them, we will obtain the T -dependence of the

electric conductivity, specific heat, Pauli paramagnetic susceptibility and NMR relaxation time (summarized in Table II).

The density of states (DOS) is given by the integral of the fermion spectral function over the momentum \mathbf{k} ;

$$\begin{aligned} -\rho_+(\omega) &= \frac{1}{\pi} \int \frac{d^3 \mathbf{k}}{(2\pi)^3} \text{Im}\overline{G}_+^R(l, \omega) \\ &= \frac{k_F^2}{c\pi^2} \int_{-\omega}^{\omega} \text{Im}\overline{G}_+^R(l, \omega) \frac{d(cl)}{2\pi}. \end{aligned} \quad (124)$$

The subscript ‘+’ refers to the DOS for the electron-type band. The following argument holds true in the same way for the hole-type band. Thus, we focus on the DOS of only the electron-type band. For small $\omega > 0$ ($\omega = 0$ corresponds to the Fermi level), the integral over the one-dimensional momentum l is dominated by the singular spectral weight near $cl = \omega$. One can see this by dividing the integral into two regions;

$$\begin{aligned} &\int_{-\omega}^{\omega} \text{Im}\overline{G}_+^R(l, \omega) \frac{d(cl)}{2\pi} \\ &= \int_{s\omega}^{\omega} \text{Im}\overline{G}_+^R(l, \omega) \frac{d(cl)}{2\pi} + \int_{-\omega}^{s\omega} \text{Im}\overline{G}_+^R(l, \omega) \frac{d(cl)}{2\pi}. \end{aligned} \quad (125)$$

Here ‘s’ is a positive constant smaller than 1. Since the integrand increases monotonically in cl for small positive ω (Fig. 3 in the main text), the second term can be bounded from above;

$$\begin{aligned} &-\int_{-\omega}^{s\omega} \text{Im}\overline{G}_+^R(l, \omega) \frac{d(cl)}{2\pi} \\ &< -\frac{(1+s)\omega}{2\pi} \text{Im}\overline{G}_+^R(cl = s\omega, \omega) = \mathcal{O}\left(\frac{1}{|\log \omega|^{\frac{3}{2}}}\right). \end{aligned} \quad (126)$$

Here we set $cl = s\omega$ in Eqs. (102,103) and assume that ω is sufficiently small;

$$\begin{aligned} \lim_{\omega \rightarrow 0} |A| &= |\log \omega| + \dots, \quad \lim_{\omega \rightarrow 0} \overline{A} = 1, \quad \lim_{\omega \rightarrow 0} \overline{B} = -\frac{\pi}{4|A|^2}, \\ \lim_{\omega \rightarrow 0} \overline{C} &= \frac{1}{\sqrt{2\alpha|A|}}, \quad \lim_{\omega \rightarrow 0} \overline{D} = -\frac{1}{\sqrt{2\alpha|A|}} \frac{\pi}{4|A|}, \\ \lim_{\omega \rightarrow 0} (\overline{A}\overline{D} - \overline{B}\overline{C}) &= -\frac{\pi}{4\sqrt{2\alpha}|\log \omega|^{\frac{3}{2}}} + \dots \end{aligned} \quad (127)$$

	R	$\frac{C_{\text{el}}}{T}$	χ_{mag}	$\frac{1}{T_1 T}$	$\rho(\omega, T=0)$
marginal-FL regime	$\sqrt{ \ln T }$	$\frac{1}{\sqrt{ \ln T }}$	$\frac{1}{\sqrt{ \ln T }}$	$\frac{1}{ \ln T }$	$\frac{1}{\sqrt{ \ln \omega }}$

TABLE II. Temperature dependence of resistivity (R), electronic contribution of specific heat C_{el} , and magnetic susceptibility χ_{mag} , and NMR relaxation time T_1 in the marginal-FL regime and the density of states near the Fermi level ($\omega = 0$) on the quantum critical point.

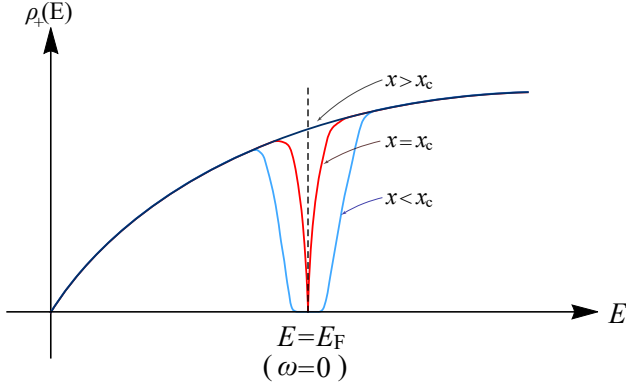


FIG. 7. Schematic picture of the density of states (DOS) for electron-type energy band near the quantum critical point. For $x > x_c$, the DOS is finite at $E = E_F$ (FL phase), while for $x < x_c$, the DOS has a finite band gap (band insulator phase). At the QCP ($x = x_c$), the DOS shows a pseudo-gap behaviour; $\rho(E) \propto 1/|\log|[E - E_F]|]^{1/2}$.

Meanwhile, for those s close to 1 ($1 - s$ is small but finite), the integrand of the first term in Eq. (125) can be approximated by the asymptotic form given in Eq. (107);

$$\int_{s\omega}^{\omega} (-) \text{Im} \bar{G}_+^R(l, \omega) \frac{d(cl)}{2\pi} \simeq \sqrt{\frac{1}{\alpha}} \frac{\pi}{2} \int_0^{(1-s)\omega} \frac{d\eta}{\eta} \frac{1}{|\log \eta|^{3/2}} = \sqrt{\frac{1}{\alpha}} \frac{1}{2} \frac{1}{|\log \omega|^{1/2}} + \dots \quad (128)$$

For small ω , Eq. (128) clearly dominates over Eq. (126). Thus, the DOS takes the following scaling form;

$$\rho_+(\omega) \propto \frac{k_F^2}{c\sqrt{\alpha}} \frac{1}{|\log \omega|^{1/2}} + \dots \quad (129)$$

Eq. (129) shows how the multiple-band Fermi system acquires a band gap when the boson system undergoes the quantum phase transition (Fig. 7). The result shows that the density of states at the Fermi level E_F ($\omega = 0$) is zero at the QCP ('pseudo-gap' behaviour).

When the temperature T is finite, ω in Eq. (129) is replaced by T and the DOS at the Fermi level becomes finite;

$$\rho_+(\omega \simeq 0, T \neq 0) \propto \frac{k_F^2}{c\sqrt{\alpha}} \frac{1}{|\log T|^{1/2}} + \dots \quad (130)$$

One can see this straightforwardly, by taking the momentum integral of the spectral function at $T \neq 0$; Eq. (109). Eq. (130) dictates that the electronic contribution to the specific heat, magnetic susceptibility and the NMR relaxation time T_1 acquire the log- T corrections at the quantum critical regime; Table II.

To evaluate the finite- T fermion's spectral function on the FS, we set $l = 0$ and use the following t in imaginary-

time Green's function in Eq. (101),

$$t = \log \left(\frac{\sqrt{\omega^2 + T^2}}{\kappa} \right). \quad (131)$$

Here we took $\hbar = k_B = 1$ for simplicity, and regarded the high temperature scale T_0 to be same as the RG scale for the frequency, κ . The choice of Eq. (131) in Eq. (101) is because the renormalization at the finite temperature must be terminated whenever either the renormalized temperature or the renormalized frequency reaches the RG scale κ . After the analytic continuation, $i\omega \rightarrow \omega + i\delta$, Eq. (101) with Eq. (131) leads to a leading-order evaluation of the retarded Green's function;

$$\begin{aligned} \bar{G}_+^{R,-1}(l=0, \omega, T \neq 0) &= (\omega + i\delta) \sqrt{1 - 2\alpha t} + \dots \\ &= \sqrt{2\alpha} \left| \log \left(\frac{\sqrt{|T^2 - \omega^2|}}{\kappa} \right) \right|^{1/2} \\ &\quad \times \left(\omega + \frac{\pi}{4} i \frac{|\omega| \theta(|\omega| - T)}{|\log(\sqrt{\omega^2 - T^2}/\kappa)|} \right) + \dots \end{aligned} \quad (132)$$

The imaginary part inside the parentheses is on the order of $T/|\log T|$ while it is zero at $\omega = 0$. This suggests that the quasi-particle life time on the FS, τ , is infinitely large within the effective model in the paper and it must be determined by other effects that are not included in the model. The most relevant effect in the low-energy scale in solids is electron scatterings by static impurities. The scattering gives a finite life time τ_{imp} at $T = 0$ and τ is primarily T -independent at low- T region;

$$\tau^{-1} \propto \tau_{\text{imp}}^{-1} + \mathcal{O}\left(\frac{T}{|\log T|}\right). \quad (133)$$

The temperature dependence of the electric conductivity can be evaluated from the Einstein relation with Eqs. (133,130);

$$\sigma = e^2 \rho D \propto \frac{e^2 k_F^2 c^{5/2} \tau_0}{g} \frac{1}{|\log T|^{1/2}}. \quad (134)$$

Here the diffusion constant D is given by the life time τ and critical velocity c of the quasi-particle on the FS, $D = c^2 \tau_0 / 3$.

The finite- T fermion's spectral function obtained from Eq. (132) has a quasi-particle delta-function peak at $\omega = 0$ (Fig. 8), being consistent with Eq. (109). The spectral function also has continuum spectrum at $|\omega| > T$. The continuum spectrum shows an asymptotic form of $1/(T |\ln \eta|^{3/2})$ for $|\omega| = T + \eta$.

APPLICATIONS TO PHYSICAL SYSTEMS

As applications of the boson-fermion coupled model, we will discuss the two physical systems (i) excitonic condensation in interacting fermion system at a fine-tuned

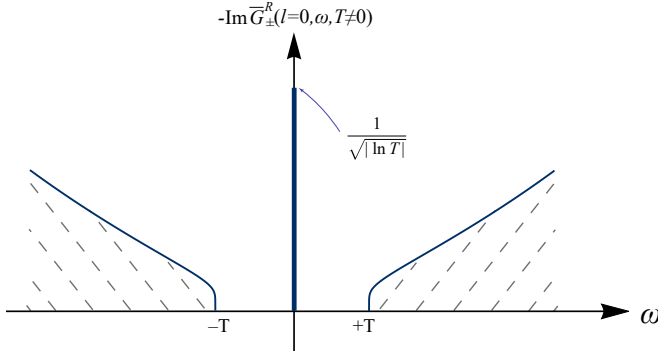


FIG. 8. Spectral function on the Fermi surface at finite temperature; $-\text{Im}G_{\pm}^R(l=0, \omega, T \neq 0)$. Plotted from Eq. (132).

‘frustrated’ point, and (ii) multiple-band electron model coupled with quantum rotor model with/without an Z_n anisotropy term ($n \geq 4$).

excitonic condensations in interacting two-bands fermion systems at a ‘frustrated’ point

Consider a two-bands interacting spinless fermion model with excitonic instability in $d = 3$;

$$\begin{aligned}
 Z &= \int \mathcal{D}a \mathcal{D}b \mathcal{D}\Phi \exp \left[- \int_0^\beta d\tau \int d^3\mathbf{x} \left\{ a^\dagger \partial_\tau a + b^\dagger \partial_\tau b \right. \right. \\
 &\quad \left. \left. - \mu_E (a^\dagger a - b^\dagger b) - \mu_0 (a^\dagger a + b^\dagger b) \right. \right. \\
 &\quad \left. \left. + H_{el}(a, b) + a^\dagger b \Phi + b^\dagger a \Phi^* - \frac{1}{g} |\Phi|^2 \right\} \right] \quad (135) \\
 &= \int \mathcal{D}\Phi \exp \left[- \int_0^\beta d\tau \int d^3\mathbf{x} \left\{ u \Phi^* \partial_\tau \Phi + v |\partial_\tau \Phi|^2 \right. \right. \\
 &\quad \left. \left. + w |\partial_{\mathbf{x}} \Phi|^2 + A |\Phi|^2 + B (|\Phi|^2)^2 + \dots \right\} \right]. \quad (136)
 \end{aligned}$$

Here $H_{el}(a, b)$ is a free (kinetic energy) part of the two-bands electron systems. a and b are field operators of the a -band (electron-type) fermion and b -band (hole-type) fermion respectively. μ_E and μ_0 are ‘staggered’ and uniform chemical potential. The staggered chemical potential μ_E is nothing but an energy difference between the electron-band energy minimum and the hole-band energy maximum (Fig. 9(a)). We call this as ‘band inversion energy’.

A repulsive interaction between the two fermions is decomposed into a coupling between an excitonic pairing field Φ , and the two fermion field operators. After an integration of the fermion fields, one would obtain the $(3+1)$ -dimensional ϕ^4 -type effective action for the excitonic field, that varies slowly in space and time (see Eq. (136)). In the absence of so-called Berry phase term, $\Phi^* \partial_\tau \Phi$, such an effective action becomes identical to the

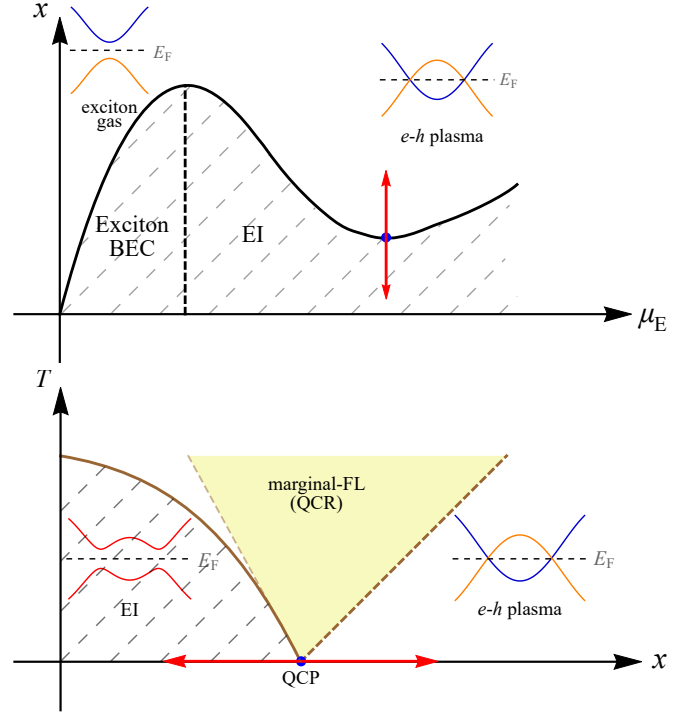


FIG. 9. a: (upper) A schematic ground state phase diagram of an interacting two-bands fermion model in the 3 spatial dimension of Eq. (135). The phase diagram is subtended by a band inversion parameter μ_E and other parameter x . The excitonic phase with the broken $U(1)$ symmetry could be identified by a region of $A < 0$ in Eq. (136), while the $U(1)$ symmetric normal phase can be identified by the other region of $A > 0$. The phase boundary between these two phases is defined by $x = X(\mu_E)$. We fine-tune μ_E at those values of μ_E where X have local minima, say $\mu_E = \mu_{E,f}$. A quantum phase transition driven by the other parameter x at $\mu_E = \mu_{E,f}$ can be well described by the effective model studied in this paper. b: (lower) A schematic T - x phase diagram associated with the quantum phase transition at $\mu_E = \mu_{E,f}$. The marginal-FL region is expected in a yellow colored region.

boson part of the effective model studied in the paper. A coefficient for the Berry phase term, u , as well as others (v, A, w, \dots) depend on microscopic parameters such as μ_E and other parameter x ;

$$u(\mu_E, x, \dots), \quad v(\mu_E, \dots), \quad A(\mu_E, \dots), \dots$$

In general, u is finite, and thus the dynamical exponent z of the boson part of the action is 2. Nonetheless, the linear coefficient u can be exactly zero when μ_E is fine-tuned at a certain point, say $\mu_E = \mu_{E,f}$,

$$u(\mu_E = \mu_{E,f}, \dots) = 0, \quad v(\mu_E = \mu_{E,f}, \dots) > 0, \quad (137)$$

where $z = 1$. A quantum phase transition at such fine-tuned point ($\mu_E = \mu_{E,f}$), that is driven by the other parameter x , is effectively well described by the fermion-boson coupled model studied in this paper, Eqs. (17,18,19,20,22).

To identify such fine-tuned critical point for μ_E , we follow an argument based on a local gauge symmetry [59]. Eq. (135) is invariant under the following local gauge transformation;

$$\begin{aligned} a^\dagger &\rightarrow a^\dagger e^{i\frac{\theta(\tau)}{2}}, \quad b^\dagger \rightarrow b^\dagger e^{-i\frac{\theta(\tau)}{2}}, \\ \Phi &\rightarrow \Phi e^{-i\theta(\tau)}, \quad \mu_E \rightarrow \mu_E - i\frac{\partial_\tau \theta}{2}. \end{aligned} \quad (138)$$

So is Eq. (136). Thus, for sufficiently small $\partial_\tau \theta(\tau)$, we could expand Eq. (136) and u , v and A in the power of $\partial_\tau \theta$, where the variation must be zero. This gives the following general relations,

$$\frac{1}{2} \frac{\partial A}{\partial \mu_E} = u, \quad \frac{1}{2} \frac{\partial u}{\partial \mu_E} = -2v. \quad (139)$$

With Eq. (139) in mind, consider a $T = 0$ phase diagram of the interacting two-bands fermion system. For simplicity, we consider a two-dimensional phase diagram subtended by μ_E and x (Fig. 9). In the $T = 0$ phase diagram, a region with $A < 0$ could be regarded as an excitonic condensate phase with the SSB of the global U(1) symmetry ($|\Phi| \neq 0$), while the other region with $A > 0$ can be regarded as a U(1) symmetric normal phase ($|\Phi| = 0$). A phase boundary between these two phases is denoted by $x = X(\mu_E)$. From Eq. (139), one can see the minima of X as a function of μ_E are the desired fine-tuned critical points with $u = 0$ and $v > 0$;

$$\begin{cases} u = 0, \quad v < 0, & \text{for } \frac{dX}{d\mu_E} = 0 \cap \frac{d^2 X}{d\mu_E^2} < 0, \\ u = 0, \quad v > 0, & \text{for } \frac{dX}{d\mu_E} = 0 \cap \frac{d^2 X}{d\mu_E^2} > 0. \end{cases} \quad (140)$$

Since the excitonic phase is suppressed as a function of x at the fine-tuned points, we call such fine-tuned values of $\mu_{E,f}$ as ‘frustrated’ points.

***sp* model coupled with a quantum rotor model**

The second physical system is a quantum rotor model coupled with two-orbital spinless fermion model. The fermion part is introduced on a 3-dimensional cubic lattice. Each lattice points has s -orbital and $p_+ \equiv p_x + ip_y$ orbital degree of freedom of the spinless fermion. The fermion Hamiltonian is described by a two-orbital tight-binding model;

$$\begin{aligned} H_{\text{sp}} &\equiv \sum_{j, \mathbf{m}} \sum_{\alpha, \beta = s, p} [\mathbb{H}]_{(j, \alpha | \mathbf{m}, \beta)} c_{j, \alpha}^\dagger c_{\mathbf{m}, \beta} \\ &\equiv \sum_j \left\{ \Delta_0 \left(-s_j^\dagger s_j + p_j^\dagger p_j \right) - t_s \sum_{\mu = x, y, z} \left(s_{j+\mu}^\dagger s_j + \text{h.c.} \right) \right. \\ &\quad \left. + t_p \left(p_{j+x}^\dagger p_j + p_{j+y}^\dagger p_j + \text{h.c.} \right) - t'_p \left(p_{j+z}^\dagger p_j + \text{h.c.} \right) \right. \\ &\quad \left. + t_{sp} \left((s_{j+x}^\dagger + i s_{j+y}^\dagger - s_{j-x}^\dagger - i s_{j-y}^\dagger) p_j + \text{h.c.} \right) \right\}, \end{aligned} \quad (141)$$

with $\mathbf{j} \equiv (j_x, j_y, j_z)$, $x \equiv (1, 0, 0)$ and so on. Here all the intra-orbital hopping integrals t_s , t_p , t'_p as well as charge energy Δ_0 are positive. When t'_p is chosen to be a negative value and the others are positive, the model becomes a prototype model for a magnetic Weyl semimetal and layered Chern insulator [56–58].

In this work, we take $t_s = t'_p = t_p = t > 0$ and $t_{sp} = t'$ for simplicity. The two energy bands are always separated by finite direct band gap;

$$E_{\pm}(\mathbf{k}) = -2tc_z \pm \sqrt{(\Delta_0 + 2t(c_x + c_y))^2 + 4t'^2(s_x^2 + s_y^2)},$$

with $c_x \equiv \cos k_x$, $s_x \equiv \sin k_x$ and so on. When $\Delta_0 - 4t > 0$, an upper energy band E_+ has an energy minimum at $(k_x, k_y, k_z) = (\pi, \pi, 0)$ and the lower energy band E_- has an energy maximum at $(k_x, k_y, k_z) = (\pi, \pi, \pi)$. When the Fermi level is set to zero, the two bands form an electron pocket and hole pocket around these extremes respectively,

$$\begin{aligned} E_{\pm} &= \pm \left(-2t + (\Delta_0 - 4t) + t(k_x^2 + k_y^2 + k_z^2) \right. \\ &\quad \left. + \frac{2t'}{\Delta_0 - 4t}(k_x^2 + k_y^2) \right) + \dots \end{aligned}$$

Note that a Fermi surface (FS) of the electron pocket around $(\pi, \pi, 0)$ and that of the hole pocket around (π, π, π) are identical in shape and size; $\mu = 0$ is the charge-neutrality point. When $\Delta_0 \gg t \gg t'$, the FS can be approximated by an isotropic Fermi surface and the two-orbital spinless fermion model can be well described by Eq. (22). Thereby, the electron and hole pockets are primarily composed of p orbital and s orbital respectively. In Eq. (141), a mixing is induced only by small t' .

The boson part takes a form of quantum rotor model on the same cubic lattice with a Z_4 anisotropy [55],

$$\begin{aligned} H_{\text{qrm}} &= \frac{\hat{L}_j^2}{2M} - J_0 \sum_{\mu = x, y} \sum_j \cos(\hat{\theta}_j - \hat{\theta}_{j+\mu}) \\ &\quad + J_{\perp} \sum_j \cos(\hat{\theta}_j - \hat{\theta}_{j+z}) - \Delta_4 \sum_j \cos(4\hat{\theta}_j) \end{aligned} \quad (142)$$

with J_0 , J_{\perp} , $\Delta_4 > 0$. θ_j represents a rotor degree of freedom defined on the cubic lattice site, taking a form of the U(1) phase variable. Δ_4 is the Z_4 anisotropy term that locks the rotor into four directions within a plane; θ_j to $0, \pm \frac{\pi}{2}, \pi$. The positive J_0 and J_{\perp} favor an antiferro-type order of the U(1) phase variable; θ_j orders in the ferro-type way within a xy plane of the cubic lattice, and it orders in the antiferro-type way along the z axis. \hat{L}_j is a momentum canonically conjugate to θ_j ;

$$[\hat{\theta}_j, \hat{L}_{\mathbf{m}}] = i\hbar \delta_{j, \mathbf{m}}. \quad (143)$$

M stands for a mass of the rotor. Larger M reduces a kinetic energy of the rotor, favoring the ordering of the

U(1) phase variable, while smaller M induces a quantum phase transition from the antiferro-type order to a quantum disorder phase. In the quantum disorder phase, the momentum takes the definite integer value at every site, $L_{\mathbf{j}} = 0$. Since the Z_4 anisotropy term is (dangerously) irrelevant at the quantum critical point [60], the quantum phase transition is well described by the (3+1)-dimensional ϕ^4 action with $z = 1$ as in Eq. (19), where $e^{i\hat{\theta}_{\mathbf{j}}}(-1)^{j_z}$ plays role of a slowly-varying $\phi(\mathbf{x})$ in Eq. (19) with $\mathbf{j} \equiv (j_x, j_y, j_z)$ being identified with \mathbf{x} [55].

coupling between rotor and sp model

In this section, we shall introduce the most natural symmetry-allowed on-site coupling between the rotor and two-orbital spinless fermions. To this end, note first that the fermion model respects a magnetic point group symmetry of $4/m\bar{m}'m'$, whose group elements are

$$C_4^z, R\sigma_x, R\sigma_y, I, \quad (144)$$

and their combinations. Here C_4^z is $\pi/2$ rotation around the z -axis, R is the time-reversal operation, σ_x, σ_y are mirror with respect to the $x = 0$ and $y = 0$ plane respectively, I is the spatial inversion. The tight-binding Hamiltonian respects the following symmetries;

$$\begin{aligned} [\mathbb{H}]_{(C_4^z(\mathbf{j})|C_4^z(\mathbf{m}))} &= \begin{pmatrix} 1 & 0 \\ 0 & -i \end{pmatrix} [\mathbb{H}]_{(\mathbf{j}|\mathbf{m})} \begin{pmatrix} 1 & 0 \\ 0 & +i \end{pmatrix} : C_4^z, \\ [\mathbb{H}^T]_{(\sigma_x(\mathbf{j})|\sigma_x(\mathbf{m}))} &= \begin{pmatrix} 1 & 0 \\ 0 & -1 \end{pmatrix} [\mathbb{H}]_{(\mathbf{j}|\mathbf{m})} \begin{pmatrix} 1 & 0 \\ 0 & -1 \end{pmatrix} : R\sigma_x, \\ [\mathbb{H}^T]_{(\sigma_y(\mathbf{j})|\sigma_y(\mathbf{m}))} &= \begin{pmatrix} 1 & 0 \\ 0 & 1 \end{pmatrix} [\mathbb{H}]_{(\mathbf{j}|\mathbf{m})} \begin{pmatrix} 1 & 0 \\ 0 & 1 \end{pmatrix} : R\sigma_y, \\ [\mathbb{H}]_{(I(\mathbf{j})|I(\mathbf{m}))} &= \begin{pmatrix} 1 & 0 \\ 0 & -1 \end{pmatrix} [\mathbb{H}]_{(\mathbf{j}|\mathbf{m})} \begin{pmatrix} 1 & 0 \\ 0 & -1 \end{pmatrix} : I. \end{aligned} \quad (145)$$

In other words, Eq. (141) is invariant under the following transformations of the creation and annihilation operators of s and p orbitals,

$$\begin{aligned} \begin{pmatrix} s \\ p \end{pmatrix} &\rightarrow \begin{pmatrix} 1 & 0 \\ 0 & +i \end{pmatrix} \begin{pmatrix} s \\ p \end{pmatrix} : C_4^z, \\ \begin{pmatrix} s \\ p \end{pmatrix} &\rightarrow \begin{pmatrix} s^\dagger & p^\dagger \end{pmatrix} \begin{pmatrix} 1 & 0 \\ 0 & -1 \end{pmatrix} : R\sigma_x, \\ \begin{pmatrix} s \\ p \end{pmatrix} &\rightarrow \begin{pmatrix} s^\dagger & p^\dagger \end{pmatrix} \begin{pmatrix} 1 & 0 \\ 0 & 1 \end{pmatrix} : R\sigma_y, \\ \begin{pmatrix} s \\ p \end{pmatrix} &\rightarrow \begin{pmatrix} 1 & 0 \\ 0 & -1 \end{pmatrix} \begin{pmatrix} s \\ p \end{pmatrix} : I \end{aligned} \quad (146)$$

with $C_4^z(A_{(\mathbf{j},\alpha|\mathbf{m},\beta)}c_{\mathbf{j},\alpha}^\dagger c_{\mathbf{m},\beta}) = A...C_4^z(c_{\mathbf{j},\alpha}^\dagger)C_4^z(c_{\mathbf{m},\beta})$, $I(Ac_{\mathbf{j},\alpha}^\dagger c_{\mathbf{m},\beta}) = AI(c_{\mathbf{j},\alpha}^\dagger)I(c_{\mathbf{m},\beta})$, and $R\sigma_\mu(Ac_{\mathbf{j},\alpha}^\dagger c_{\mathbf{m},\beta}) = AR\sigma_\mu(c_{\mathbf{m},\beta})R\sigma_\mu(c_{\mathbf{j},\alpha}^\dagger)$.

In the following, we introduce an on-site coupling between the two-orbital fermions and rotor, that respects all (or part of) these magnetic point group symmetry operations. To do so, we consider two physical cases, (i) when the rotor on each site has the same symmetry as x and y -components of electric dipole; $e^{i\theta_{\mathbf{j}}} \sim E_x(\mathbf{j}) + iE_y(\mathbf{j})$, and (ii) when the rotor has the same symmetry as the x and y -components of magnetic dipole; $e^{i\theta_{\mathbf{j}}} \sim B_x(\mathbf{j}) + iB_y(\mathbf{j})$.

when rotor is electric dipole

Consider the first case, where real and imaginary part of $e^{i\theta_{\mathbf{j}}}$ has the same symmetry as the x and y components of the electric dipole moment defined at \mathbf{j} respectively. Under the symmetry operations of $4/m\bar{m}'m'$, the rotor degree of freedom will be transformed as follows,

$$\begin{aligned} e^{i\theta_{\mathbf{j}}} &\rightarrow e^{i(\theta_{\mathbf{j}} + \frac{\pi}{2})} : C_4^z, \quad e^{i\theta_{\mathbf{j}}} \rightarrow e^{i\theta_{\mathbf{j}}} : R, \\ e^{i\theta_{\mathbf{j}}} &\rightarrow e^{-i\theta_{\mathbf{j}}} : \sigma_y, \quad e^{i\theta_{\mathbf{j}}} \rightarrow e^{i(\pi - \theta_{\mathbf{j}})} : \sigma_x, \\ e^{i\theta_{\mathbf{j}}} &\rightarrow -e^{i\theta_{\mathbf{j}}} : I, \quad e^{i\theta_{\mathbf{j}}} \rightarrow -e^{-i\theta_{\mathbf{j}}} : R\sigma_x, \\ e^{i\theta_{\mathbf{j}}} &\rightarrow e^{-i\theta_{\mathbf{j}}} : R\sigma_y. \end{aligned} \quad (147)$$

Thus, the simplest on-site coupling between the electric dipole and the fermions that respects all the magnetic point group symmetry of $4/m\bar{m}'m'$ is as follows,

$$H_{f-b} = \sum_{\mathbf{j}} \left(e^{-i\hat{\theta}_{\mathbf{j}}} s_{\mathbf{j}}^\dagger p_{\mathbf{j}} + e^{i\hat{\theta}_{\mathbf{j}}} p_{\mathbf{j}}^\dagger s_{\mathbf{j}} \right). \quad (148)$$

In the presence of this on-site fermion-boson coupling, the slowly varying $\phi(\mathbf{x} \simeq \mathbf{j}) = e^{-i\hat{\theta}_{\mathbf{j}}}(-1)^{j_z}$ couples between the electron and hole pockets in the same form as in Eq. (20).

when rotor is magnetic dipole

Consider the second case, where real and imaginary part of $e^{i\theta_{\mathbf{j}}}$ has the same symmetry as the x and y components of the magnetic dipole moment defined at \mathbf{j} . Under the magnetic point group symmetry operations, the rotor degree of freedom will be transformed as follows,

$$\begin{aligned} e^{i\theta_{\mathbf{j}}} &\rightarrow e^{i(\theta_{\mathbf{j}} + \frac{\pi}{2})} : C_4^z, \quad e^{i\theta_{\mathbf{j}}} \rightarrow -e^{i\theta_{\mathbf{j}}} : R, \\ e^{i\theta_{\mathbf{j}}} &\rightarrow e^{i(\pi - \theta_{\mathbf{j}})} : \sigma_y, \quad e^{i\theta_{\mathbf{j}}} \rightarrow e^{-i\theta_{\mathbf{j}}} : \sigma_x, \\ e^{i\theta_{\mathbf{j}}} &\rightarrow e^{i\theta_{\mathbf{j}}} : I, \quad e^{i\theta_{\mathbf{j}}} \rightarrow -e^{-i\theta_{\mathbf{j}}} : R\sigma_x, \\ e^{i\theta_{\mathbf{j}}} &\rightarrow e^{-i\theta_{\mathbf{j}}} : R\sigma_y. \end{aligned} \quad (149)$$

Thus the on-site coupling in Eq. (148) is symmetrically allowed by $C_4^z, R\sigma_x$ and $R\sigma_y$, while it is disallowed by I . In other words, the coupling of Eq. (20) is allowed by

a subgroup of $4/m\bar{m}'m'$: $4m'm'$. The group elements of and their combinations.
the magnetic point group of $4m'm'$ are

$$C_4^z, R\sigma_x, R\sigma_y, \quad (150)$$